



# The effect of climate change on the simulated streamflow of six Canadian rivers based on the CanRCM4 regional climate model

Vivek. K. Arora<sup>1</sup>, Aranildo Lima<sup>1</sup>, Rajesh Shrestha<sup>2</sup>

<sup>1</sup>Canadian Centre for Climate Modelling and Analysis, Climate Research Division, Environment Canada, Victoria, BC, Canada

<sup>2</sup>Climate Research Division, Environment and Climate Change Canada, Victoria, BC, Canada

1

2 *Correspondence to:* Vivek K. Arora (vivek.arora@ec.gc.ca)



3 **Abstract**

4

5 The effect of climate change is investigated on the hydro-climatology of six major Canadian rivers  
6 (Mackenzie, Yukon, Columbia, Fraser, Nelson, and St. Lawrence), in particular streamflow, by  
7 analyzing results from the historical and future simulations (RCP 4.5 and 8.5 scenarios) performed  
8 with the Canadian regional climate model (CanRCM4). Streamflow is obtained by routing runoff  
9 using river networks at 0.5° resolution. Of these six rivers, Nelson and St. Lawrence are the most  
10 regulated. As a result, the streamflow at the mouth of these rivers shows very little seasonality.  
11 Additionally, the Great Lakes significantly dampen the seasonality of streamflow for the St.  
12 Lawrence River. Mean annual precipitation (P), evaporation (E), runoff (R), and temperature  
13 increase for all six river basins considered and the increases are higher for the more fossil fuel-  
14 intensive RCP 8.5 scenario. The only exception is the Nelson River basin for which the simulated  
15 runoff increases are extremely small. The hydrological response of these rivers to climate  
16 warming is characterized by their existing climate states. The northerly Mackenzie and Yukon  
17 River basins show a decrease in evaporation ratio (E/P) and an increase in runoff ratio (R/P) since  
18 the increase in precipitation is more than enough to offset the increase in evaporation associated  
19 with increasing temperature. For the southerly Fraser and Columbia River basins, the E/P ratio  
20 increases, and the R/P ratio decreases due to an already milder climate in the Pacific north-  
21 western region. The seasonality of simulated monthly streamflow is also more affected for the  
22 southerly Fraser and Columbia Rivers than for the northerly Mackenzie and Yukon Rivers as snow  
23 amounts decrease and snowmelt occurs earlier. The streamflow seasonality for the Mackenzie  
24 and Yukon rivers is still dominated by snowmelt at the end of the century even in the RCP 8.5  
25 scenario. The simulated streamflow regime for the Fraser and Columbia Rivers shifts from a  
26 snow-dominated to a hybrid/rainfall-dominated regime towards the end of this century in the  
27 RCP 8.5 scenario. While we expect the climate change signal from CanRCM4 to be higher than  
28 other climate models, owing to the higher-than-average climate sensitivity of its parent global  
29 climate model, the results presented here provide a consistent overview of hydrological changes  
30 across six major Canadian river basins in response to a warmer climate.

31



## 32 **1. Introduction**

33           As the global population and the standard of living increases so does the strain on  
34 freshwater resources. The natural availability of water is determined by the balance between  
35 precipitation (P) and evaporation (E) (although the term evapotranspiration is more correct).  
36 When precipitation exceeds evaporation, which is determined primarily by available energy, the  
37 water that doesn't evaporate or transpire (either at the surface or after infiltration into the soil)  
38 termed runoff (R) is carried by the rivers to the oceans. The seasonality of precipitation, its  
39 partitioning into snow and rainfall, and the seasonality of snowmelt and evaporation, all of which  
40 are determined by the climate in a given catchment or a river basin eventually determine the  
41 seasonality of runoff. As anthropogenic climate change progresses, changes in the mean annual  
42 amounts and the seasonality of these different water budget components will lead to  
43 corresponding changes in runoff (Trenberth et al., 2007). Changes in precipitation extremes are  
44 also expected to lead to corresponding changes in the extremes of streamflow. The changes in  
45 streamflow have implications for floods and power generation. While runoff is expressed in  
46 similar units to precipitation and evaporation (depth of water per unit time, e.g. mm/s or  
47 m/year), streamflow is the volume of water generated per unit time and requires multiplication  
48 with the area over which runoff is generated. Streamflow is also routed down the river network  
49 which introduces a time lag and attenuation of the peak runoff. As a result, the streamflow is  
50 expressed in units of volume per unit time (e.g. m<sup>3</sup>/s or km<sup>3</sup>/year).

51           Output from climate and Earth system models (ESMs) remains the primary source of  
52 information for evaluating climate change impacts. Current approaches that rely on information  
53 generated by ESMs, to obtain an estimate of how future streamflow may potentially change, may



54 be classified into two broad categories. The first approach uses simulated runoff directly from  
55 the land surface component of single or multiple climate models which may be routed  
56 downstream to obtain streamflow at the mouths of river basins and at different points along a  
57 given river network (Miller and Russell, 1992; Arora and Boer, 2001; Zhang et al., 2014). Using  
58 direct runoff output from climate models has the benefit that the calculated changes in runoff  
59 are physically consistent with the altered radiative balance of the Earth in response to increases  
60 in the concentrations of greenhouse gases (GHGs). The corresponding changes in the general  
61 circulation of the atmosphere result in the associated changes in near-surface temperature,  
62 precipitation, and the hydrological cycle. This approach suffers from three limitations – 1) the  
63 biases in the climate simulated by the climate model, 2) the fact that the land surface  
64 components of climate models are not calibrated for a given river basin but rather designed to  
65 operate in a reasonably realistic way over the whole globe, and 3) the coarse resolution of global  
66 climate models (GCMs). The last limitation is partially addressed when data from finer-resolution  
67 regional climate models is used. The biases in the simulated climate do affect the simulated  
68 runoff for the current climate. Despite this, however, the response to climate change is relatively  
69 robust and there is useful information in the simulated change that can be used to inform  
70 adaptation measures. The second approach attempts to overcome these limitations by  
71 downscaling and/or bias-correcting climate from climate models for future scenarios and uses  
72 that to drive a well-calibrated hydrological model for given catchments or river basins (Ismail et  
73 al., 2020; Yoosefdoost et al., 2022; Gosling et al., 2011; Miller et al., 2021). The second approach  
74 is more prevalent for watershed to regional scale impacts and adaptation studies. Given the large  
75 effort involved in downscaling and bias-correcting raw climate data from climate models, most



76 current impact studies use downscaled and bias-corrected data put together by other groups  
77 rather than specifically doing this for their project. Recent examples include the downscaled and  
78 bias-corrected climate data for the conterminous United States (Thrasher et al., 2013) based on  
79 climate model output from the fifth phase of the Coupled Model Intercomparison Project  
80 (CMIP5), and statistically downscaled and bias-corrected data based from five CMIP5 models,  
81 available at the global scale, tailored to the requirements of the Inter-Sectoral Impact Model  
82 Intercomparison Project (ISIMIP) (Lange, 2019). Both these datasets have found large  
83 applications in the impacts and adaptation community. The processes of downscaling and bias  
84 correction are distinct, and they both have their inherent limitations. There are several examples  
85 of the limited ability of bias-correction to correct and to downscale variability, that bias-  
86 correction can potentially cause implausible climate change signals, and there remain  
87 uncertainties, substantial contradictions, and sensitivity to assumptions between the different  
88 downscaling methods (Maraun et al., 2017; Maraun, 2016; Hewitson et al., 2014). Well-calibrated  
89 hydrological models are generally suitable for a given catchment or a river basin but their  
90 application has not been extended to large-scale global or regional hydrologic modelling studies  
91 since it is typically not straightforward to tune model parameters for all river basins. In the end,  
92 both approaches are complementary to each other.

93 Future hydrologic projections using the second approach (hydrological modes driven by  
94 statistically downscaled and bias-adjusted climate models) are available for selected river basins  
95 in Canada. The results over the Prairies and British Columbia (Shrestha et al., 2021b; Sobie and  
96 Murdock, 2022) generally indicate shorter snow cover duration, earlier snowmelt, and reduced  
97 annual maximum snow water equivalent as the climate warms. Streamflow projections across



98 Canada generally indicate earlier occurring snowmelt-driven peak flow, increased winter flow,  
99 and decreased summer flow (MacDonald et al., 2018; Shrestha et al., 2019; Islam et al., 2019;  
100 Dibike et al., 2021; Budhathoki et al., 2022). Annual streamflow is generally projected to increase,  
101 with higher increases in the northern basins (Bonsal et al., 2020; Stadnyk et al., 2021). However,  
102 these projections are based on different climate and hydrological models, downscaling methods,  
103 emissions scenarios, and future periods, and no consistent set of projections is available across  
104 all major river basins of Canada.

105 In this study, we have used the first approach to provide a consistent set of projections  
106 across all major river basins of Canada. We investigate the effect of climate change on the annual,  
107 monthly, and daily streamflow characteristics of six major Canadian rivers (Mackenzie, Yukon,  
108 Columbia, Fraser, Nelson, and St. Lawrence) using runoff output from simulations performed  
109 with version 4 of the Canadian Regional Climate Model (CanRCM4). The river basins of the Yukon  
110 and Columbia Rivers cover part of the United States of America as well. We used daily runoff  
111 generated from CanRCM4 for the historical period and for the two future scenarios  
112 (representative concentration pathways (RCP) 4.5 and 8.5). The spatial resolution of runoff data  
113 from CanRCM4 is  $0.22^\circ$  which is equivalent to about 12 km at  $60^\circ$  N (Canada lies between  
114 approximately  $42^\circ$ N and  $83^\circ$ N). Additionally, we utilized a large ensemble (50 realizations) of the  
115 CanRCM4 (CanRCM4-LE) at  $0.44^\circ$  resolution to quantify uncertainties associated with internal  
116 variability. We then routed this runoff through river networks at  $0.5^\circ$  resolution to evaluate  
117 streamflow at the mouths of major Canadian rivers. The Mackenzie, Yukon, and Fraser Rivers are  
118 somewhat less regulated than the heavily regulated Nelson, Columbia, and St. Lawrence Rivers.  
119 The routing scheme used here does not take into account dams and reservoirs and therefore the



120 modelled streamflow represents natural streamflow. This aspect is discussed in more detail in  
121 Section 2.0

## 122 **2. Models and data**

123 Equation (1) summarizes the water balance over a given grid cell or a river basin for a  
124 given timescale.

$$125 \qquad \qquad \qquad P = E + R + \Delta S \qquad \qquad \qquad (1)$$

126 where  $\Delta S$  is the change in water storage including that in soil moisture, snow, and the canopy  
127 water storage combined. When a system is in equilibrium, at annual or longer timescales  $\Delta S =$   
128 0 and  $P = E + R$ .  $\Delta S$ , however, may not be zero even over long timescales when a system is not  
129 in equilibrium e.g., when snow is accumulating or is melting consistently. We evaluated P, E, and  
130 R components of equation (1) simulated by CanRCM4 for each of the six river basins, considered  
131 in this analysis, and routed R to obtain streamflow at the river mouths.

132

### 133 **2.1 The Canadian Regional Climate Model (CanRCM4)**

134 CanRCM4 uses the fourth-generation Canadian atmospheric physics (CanAM4) package  
135 (von Salzen et al., 2013), which is the product of a multi-decadal program of climate model  
136 development at the Canadian Centre for Climate Modelling and Analysis (CCCma), a section  
137 within Environment and Climate Change Canada. The CanAM4 atmospheric physics package is  
138 also used in CanESM2 (Arora et al., 2011) which contributed results to the CMIP5. The difference  
139 between CanRCM4 and CanESM2, other than the former being a regional climate model and the  
140 latter being a comprehensive global ESM, is that CanRCM4 employs the limited-area



141 configuration of the Global Environmental Multiscale (GEM) model (Côté et al., 1998), which uses  
142 a semi-Lagrangian dynamical core for advection in the atmosphere and is developed by  
143 Environment and Climate Change Canada's Recherche en Prévision Numérique (RPN) where it is  
144 used both for global and regional numerical weather prediction. CanESM2 on the other hand  
145 uses a spectral dynamical core for advection in the atmosphere. CanRCM4 is driven at its  
146 boundaries with data from its parent model (CanESM2). An overview and technical details of the  
147 coordinated global and regional climate modelling effort used to develop the CanESM2-CanRCM4  
148 system are described in detail by Scinocca et al. (2016). Results from the model's North American  
149  $0.22^\circ$  domain, for a single ensemble member, are primarily used here. In addition, we also used  
150 runoff from CanRCM4  $0.44^\circ$  resolution simulations for the North American domain because of  
151 the availability of a large ensemble (LE) of 50 members (CanRCM4 LE) (ECCC, 2018). The large  
152 ensemble simulations allow the consideration of CanRCM4's internal variability, which is an  
153 intrinsic property of the climate system and models, that is largely irreducible and could account  
154 for a large fraction of the inter-GCM model spread (Deser et al., 2020). The results used here  
155 from CanRCM4's form part of its contribution to the coordinated regional climate downscaling  
156 experiment (CORDEX) effort. The North American domain of CanRCM uses a rotated latitude-  
157 longitude projection with the North Pole at longitude  $83^\circ$  E and latitude  $42.5^\circ$  N, as opposed to  
158 the geographic North Pole (latitude  $90^\circ$  N).

159         The land surface component in the physics component of CanAM4 is the coupled CLASS-  
160 CTEM model. The physical processes are based on the Canadian Land Surface Scheme (CLASS)  
161 (Verseghy, 1991; Verseghy et al., 1993), and biogeochemical processes (which simulate  
162 vegetation as a dynamic component of the climate system) are based on the Canadian Terrestrial





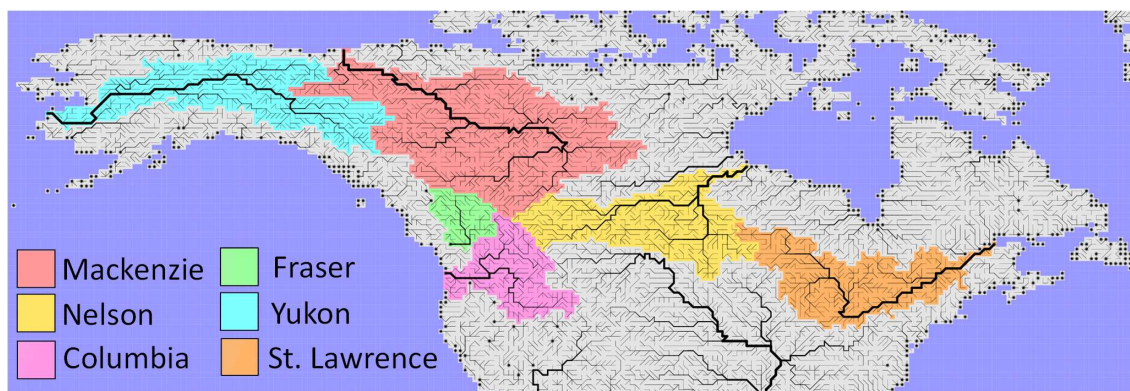
163 Ecosystem Model (CTEM) (Arora and Boer, 2005, 2003). The configuration of CLASS-CTEM used  
164 in CanESM2 and CanRCM4 uses three soil layers with thicknesses of 0.10, 0.25, and 3.75 m. Liquid  
165 and frozen soil moisture contents, and soil temperature, are determined prognostically for the  
166 three soil layers. The temperature, albedo, mass, and density of a single-layer snow pack (when  
167 environmental conditions permit snow to exist) are also prognostically modelled. Surface runoff  
168 is generated in CLASS when precipitation intensity exceeds infiltration capacity and when the top  
169 soil layer is saturated. The rainwater and snow melt that infiltrates the soil is available for soil  
170 evaporation and transpiration. Any remaining water percolates down the soil profile and comes  
171 out at the bottom of the soil profile and is termed drainage. Combined surface runoff and  
172 drainage constitute total runoff. Like most land surface components of ESMs, CLASS does not  
173 include a groundwater representation. Surface runoff and drainage components of runoff from  
174 CLASS are used as input into a large-scale river routing scheme to route runoff and obtain  
175 streamflow at the mouth of the rivers considered in this study as explained in the next section.

## 176 **2.2 Variable velocity routing model**

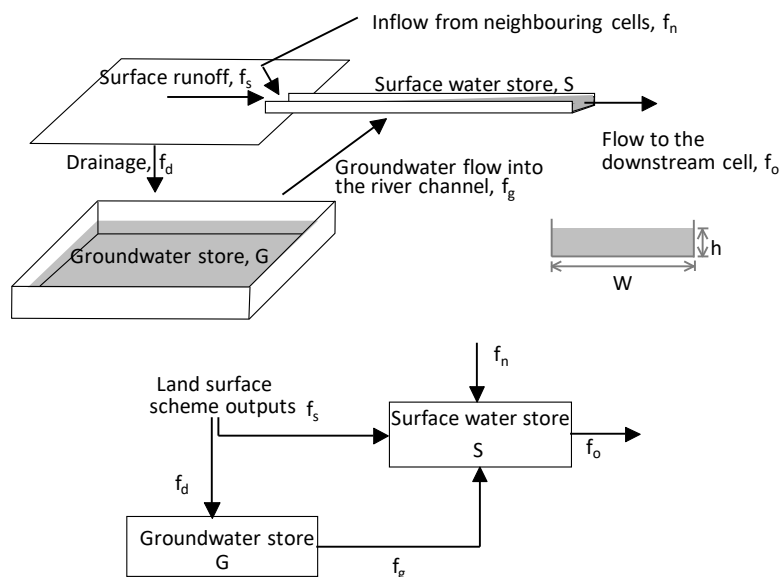
177 The variable velocity river routing scheme of Arora and Boer (1999) that is implemented  
178 in the family of Canadian ESMs (CanESMs) (Arora et al., 2009, 2011; Swart et al., 2019) is used to  
179 route daily runoff from CanRCM4. This routing scheme has been implemented in various versions  
180 of CanESMs at a spatial resolution of  $2.81^\circ$  since the year 2000. For this study, the routing scheme  
181 was implemented at a spatial resolution of  $0.5^\circ$ . The reason for using river routing at  $0.5^\circ$   
182 resolution instead of scaling river networks to the  $0.22^\circ$  rotated latitude-longitude projection of  
183 CanRCM4 's North American domain is that scaling river networks is a non-trivial task that cannot  
184 be fully automated (Arora and Harrison, 2007). In contrast, conservatively regridding runoff from



185 one spatial resolution to another is a straightforward process. The routing scheme needs river  
186 flow directions and these are obtained from the Total Integrating Runoff Pathways (TRIP) dataset  
187 (<http://hydro.iis.u-tokyo.ac.jp/~taikan/TRIPDATA/TRIPDATA.html>, last accessed July 2023) of Oki  
188 and Sud (1998). The TRIP data are available at the regular latitude-longitude grid with the  
189 geographic North Pole at its usual location ( $90^{\circ}$  N). Figure 1 shows the river networks at  $0.5^{\circ}$   
190 resolution based on TRIP data which also identifies the six river basins investigated in this study.  
191 The Fraser River (identified by the light green colour) appears to have a river mouth over land.  
192 This is because the Fraser River drains into the narrow Strait of Georgia which is not resolved at  
193 the  $0.5^{\circ}$  resolution of the TRIP dataset. In addition, the TRIP data set does not resolve any inland  
194 lakes and provides river flow directions over grid cells that are lakes. This is in fact helpful because  
195 it avoids discontinuities in the river network.



196  
 197 **Figure 1:** River flow networks at 0.5° resolution used in this study. The major river basins for  
 198 which streamflow and runoff are analyzed in this study are also identified.  
 199



200  
 201 **Figure 2:** Schematic of the Arora and Boer (1999) river routing scheme used in this study to route  
 202 runoff simulated by CanRCM4.

203

204 Figure 2 shows the schematic of the routing scheme which uses surface runoff and  
 205 drainage outputs from the land surface scheme. The routing scheme is described briefly here and



206 more details can be found in Arora and Boer (1999). The river channel is assumed to be  
207 rectangular and the width ( $W$ ) of the river at every point along the river network is specified a  
208 priori. This river width is calculated based on its geomorphological relationship with mean annual  
209 discharge. The surface runoff contributes directly to the surface water store which is essentially  
210 the amount of water in the rectangular river channel between two grid cells. The flow velocity  
211 ( $V$ ) is calculated using the Mannings formula.

$$212 \quad V = \frac{1}{r} R^{2/3} S^{1/2} = \frac{1}{r} \left( \frac{A}{P} \right)^{2/3} S^{1/2} = \frac{1}{r} \left( \frac{Wh}{W+2h} \right)^{2/3} S^{1/2} \quad (2)$$

213 where  $r$  is the Mannings roughness coefficient (a default value of 0.04 is used),  $A$  is the area of  
214 the river channel,  $P$  is the wetted perimeter, and  $h$  is the depth of water in the channel. Multiplied  
215 with the river's cross-sectional area, the time-varying velocity determines the output discharge  
216 from the surface water store of the current grid cell to the river channel of the downstream grid  
217 cell. The drainage from the bottommost soil layer contributes to the groundwater store which  
218 eventually contributes to the surface water store in the same grid cell. The delay in the  
219 groundwater store is based on the dominant soil texture type and is set to 10, 35, and 65 days if  
220 the dominant soil type in each grid cell is sand, silt, and clay, respectively, following Arora and  
221 Boer (1999). Both the depth and velocity of the water in the river channel are prognostic variables  
222 and evolve in time depending on the amount of water in the river channel.

223 The routing scheme used here does not consider the flow regulation effect of dams and  
224 reservoirs. It, however, does consider the effect of lakes and ice jams in a simple manner. The  
225 global lake data set from Kourzeneva et al. (2012) is used which prescribes the fractional coverage  
226 of sub-grid lakes and the five Laurentian Great Lakes (Lakes Superior, Michigan, Huron, Ontario,



227 and Erie). In particular, the flow at the mouth of the St. Lawrence River is affected significantly  
228 by the Great Lakes. The hydraulic residence of water in the Great Lakes varies from about 2 years  
229 for Lake Erie to about 200 years for Lake Superior (Quinn, 1992). As a result, even in the absence  
230 of anthropogenic flow regulation for the St. Lawrence River, we expect the streamflow at its  
231 mouth to show very little seasonality compared to the usual spring peak of Canadian rivers  
232 dominated by snowmelt. The simple approach used here delays the streamflow flowing into a  
233 grid cell with a lake fraction greater than 60% using an e-folding time scale of 300 days similar to  
234 the treatment of the groundwater reservoir (Figure 2) (Arora and Boer, 1999). For the St.  
235 Lawrence River, the effect of delay caused by the Great Lakes is much larger than that of the  
236 anthropogenic flow regulation.

237 Ice jams and breakups are complex thermal and mechanical events and therefore  
238 challenging to model. They occur on all Canadian rivers with varying degrees and depend on  
239 winter temperatures, the river bathymetry, and the physical and geomorphological conditions of  
240 rivers (Prowse, 1986; Beltaos, 2000). The winter freezing of river water inevitably leads to a slow  
241 down of river flow velocity. When water cannot move downstream, upstream flooding results.  
242 Here, we have used a simple approach that increases Manning's roughness coefficient (a value  
243 of 0.08 is used) for the Mackenzie and the Yukon Rivers (which are the most northerly and  
244 therefore affected the most by ice jams) for the period January to June. Chen and She (2020)  
245 report the trend in river ice breakup dates for the Mackenzie and Yukon Rivers to be around -0.3  
246 and -1.3 days/decade for the 1950-2016 period, where the negative sign indicates that the ice  
247 breakup is occurring earlier. Assuming the same trend, the breakup dates would occur about 2.5  
248 and 11 days earlier towards the end of this century, respectively, for the Mackenzie and Yukon



249 rivers. This simple approach reduces the river flow velocity during the months that are most  
250 affected by river ice jams. Although this is not a perfect nor a complete approach this simple  
251 treatment allows to improve the streamflow seasonality for the Mackenzie and Yukon rivers. For  
252 the southerly Fraser and Columbia rivers such treatment wasn't necessary. Consideration of a  
253 higher roughness coefficient for the St. Lawrence River to account for ice jams does not affect its  
254 streamflow's seasonality (or rather lack of it) which is overwhelmingly determined by the delay  
255 and storage caused by the Great Lakes.

### 256 **2.3 Modelled and observation-based data**

257 The CMIP5 historical simulation covers the period 1850-2005 and the future scenarios  
258 cover the period 2006-2100. We used daily runoff from CanRCM4 from its 0.22° North American  
259 domain for the 20 years 1986-2005 from one ensemble member of the historical simulation and  
260 for the 20 years 2081-2100 from one ensemble member each for the two future scenarios (RCP  
261 4.5 and RCP 8.5, Moss et al. (2010)). The RCP 8.5 is the highest baseline emissions scenario where  
262 future development is based on continuous fossil-fuel development. As a result, CO<sub>2</sub> emissions  
263 and concentrations increase throughout the 21<sup>st</sup> century and CO<sub>2</sub> concentration in the year 2100  
264 is around 1100 ppm. RCP 4.5 is a moderate emissions scenario in which emissions peak around  
265 2040 and then decline: as a result CO<sub>2</sub> somewhat stabilizes to around 550 ppm by the year 2100.  
266 Since the CanRCM4 data are available on a rotated latitude-longitude grid and the river routing  
267 is performed on a regular latitude-longitude grid (following the TRIP data) the runoff data from  
268 CanRCM4 are conservatively regridded to the global 0.5° grid using climate data operators (CDO)  
269 (<https://code.mpimet.mpg.de/projects/cdo/embedded/index.html#x1-7170002.12.5>, last  
270 accessed Dec 2023). These runoff data are then used as input into the routing model. The 20-



271 year runoff data (1986-2005 for the historical simulation, and 2081-2100 for the future scenarios)  
272 are concatenated into a 40-year time series for each simulation (historical, RCP 4.5, and RCP 8.5).  
273 These data are then input into the routing model and the last 20 years of simulated streamflow  
274 are then analyzed. The 20-year spin-up is sufficient to allow the surface and groundwater stores  
275 to fill up and reach equilibrium. The simulated precipitation and temperature from CanRCM4 are  
276 compared against observation-based data from the CRU TS 4.07 product (Harris et al., 2020).

277         The simulated streamflow is compared against observation-based estimates obtained  
278 from the Global Runoff Data Centre (GRDC) for the stations that are closest to the river mouths.  
279 Table 1 lists the drainage areas of all rivers considered in this study as discretized in the TRIP data  
280 set and at the stations closest to the river mouth. For the Columbia River, which is heavily  
281 regulated, we obtain an estimate of the naturalized flow with no regulation and no irrigation  
282 provided by the Bonville Power Administration (BPA) for the station VAN (near Vancouver,  
283 Washington, USA) ([https://www.bpa.gov/energy-and-services/power/historical-streamflow-](https://www.bpa.gov/energy-and-services/power/historical-streamflow-data)  
284 [data;https://www.bpa.gov/-/media/Aep/power/historical-streamflow-reports/historic-](https://www.bpa.gov/-/media/Aep/power/historical-streamflow-reports/historic-streamflow-nrni-flows-1929-2008-corrected-04-2017.csv)  
285 [streamflow-nrni-flows-1929-2008-corrected-04-2017.csv](https://www.bpa.gov/-/media/Aep/power/historical-streamflow-reports/historic-streamflow-nrni-flows-1929-2008-corrected-04-2017.csv), last accessed July 2023). The drainage  
286 area of the Columbia River upstream of the VAN station is 616960 km<sup>2</sup> and does not include  
287 discharge contributions from three tributaries (Willamette, Cowlitz, and Lewis Rivers). Of these  
288 three tributaries, the contribution from Willamette is the largest. We obtained naturalized  
289 streamflow for the Willamette River at the station SVN (drainage area 25,600 km<sup>2</sup>) also from  
290 BPA's website ([https://www.bpa.gov/-/media/Aep/power/historical-streamflow-](https://www.bpa.gov/-/media/Aep/power/historical-streamflow-reports/correction-20220801.zip)  
291 [reports/correction-20220801.zip](https://www.bpa.gov/-/media/Aep/power/historical-streamflow-reports/correction-20220801.zip), from the file SVN6ARF\_daily\_COR.xlsx) and added it to the  
292 naturalized streamflow at the station VAN. This yields naturalized streamflow for the entire



293 Columbia River basin, except the smaller Cowlitz, and Lewis Rivers, and represents a drainage  
294 area of 642,560 km<sup>2</sup> (see Table 1).

295 The Nelson River is affected by two large lakes, Lake Winnipeg and Lake Manitoba, and in  
296 addition, it is also heavily regulated. It currently has five dams towards the end of its journey as  
297 it flows into Hudson Bay. There are no upstream gauging stations close to the first upstream dam.  
298 In addition, water is also diverted from Churchill to the Nelson River. We were unable to obtain  
299 naturalized flow for the Nelson River. Due to anthropogenic flow regulation on the Nelson River,  
300 the present-day streamflow shows very little seasonality (as shown later). As a result, we do not  
301 evaluate the simulated monthly streamflow for the Nelson River and focus only on its mean  
302 annual value.

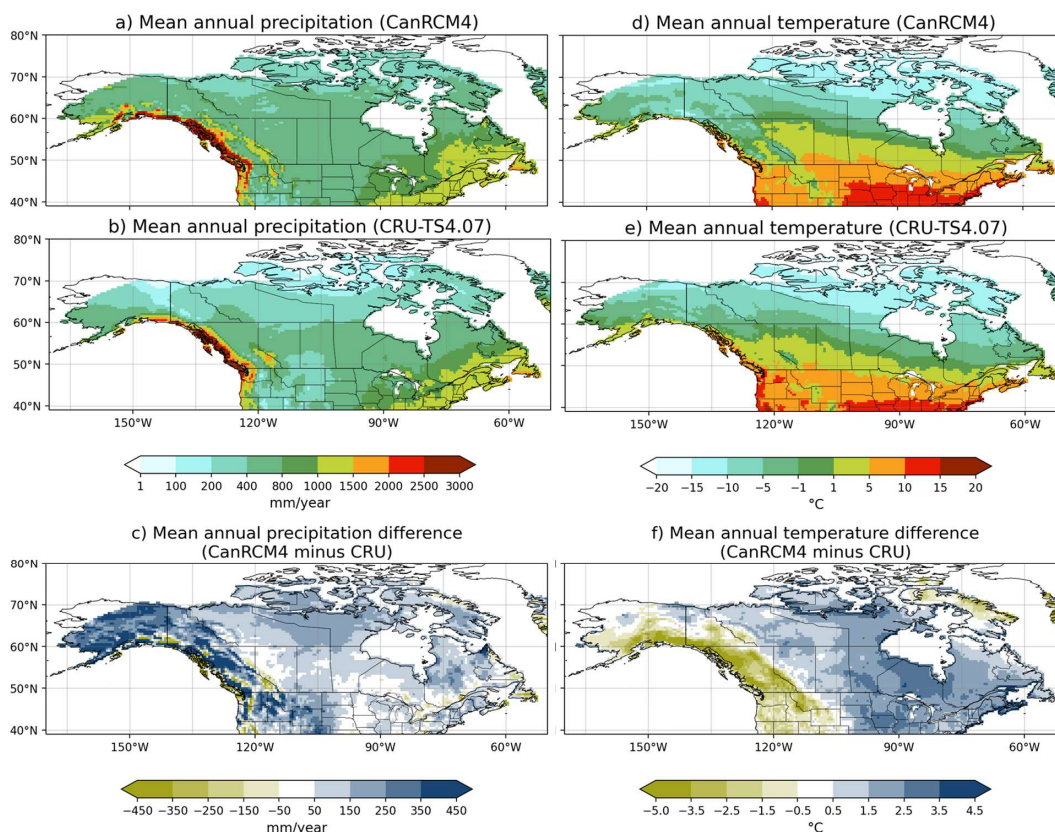
303 **Table 1:** Comparison of river basin areas as represented in the TRIP data and at the gauging  
304 station closest to the river mouth for the river basins considered in this study as obtained from  
305 the GRDC.

306  
307

River basin	River basin area (million km <sup>2</sup> )		Gauging station
	in the TRIP dataset	at the gauging station closest to the river mouth	
Mackenzie	1.74	1.66	Arctic red river
Yukon	0.85	0.83	Pilot Station
Columbia	0.66	0.64	See section 2.3
Fraser	0.23	0.22	Hope
Nelson	1.07	1.06	Long Spruce generating station
St. Lawrence	1.11	0.77	Cornwall, Ontario

308  
309  
310  
311





312

313 **Figure 3:** Comparison of CanRCM4 simulated precipitation (left column) and temperature (right  
314 column) with observation-based estimates from the CRU TS 4.07 dataset for the period 1986-  
315 2005.

316

### 317 3. Results

#### 318 3.1 Present-day precipitation, temperature, and streamflow

319 Figure 3 compares the mean annual precipitation (left column) and temperature (right  
320 column) simulated by CanRCM4 to observation-based estimates from the CRU TS 4.07 dataset  
321 (referred to as CRU from here on) for the 1986-2005 period. Although the six river basins  
322 considered in this study do not cover the entire Canadian region, for completeness the plots are



323 shown for the whole of Canada and south up to 39 °N to include the southern edge of the  
324 Columbia River basin. In Figure 3, while CanRCM4 broadly simulates the geographical distribution  
325 of temperature and precipitation reasonably realistically, there are differences compared to the  
326 CRU dataset. CanRCM4 generally simulates higher precipitation over Canada and more so to the  
327 west of the Rockies (Figure 3c) compared to observations. The model simulates cooler than  
328 observed temperatures to the west of the Rockies and higher than observed temperatures to the  
329 east of the Rockies (Figure 3f). This is likely related to the representation of topography in the  
330 model. The overall somewhat higher precipitation in CanRCM4 over North America is also noted  
331 by Alaya et al. (2019) who compared probable maximum precipitation (PMP) calculated using  
332 CanRCM4 data and compared it to estimates based on several reanalysis. Alaya et al. (2019)  
333 concluded that among the three reanalyses they considered, CanRCM4 compared best with the  
334 National Centre for Environmental Prediction's (NCEP) Climate Forecast System Reanalysis.

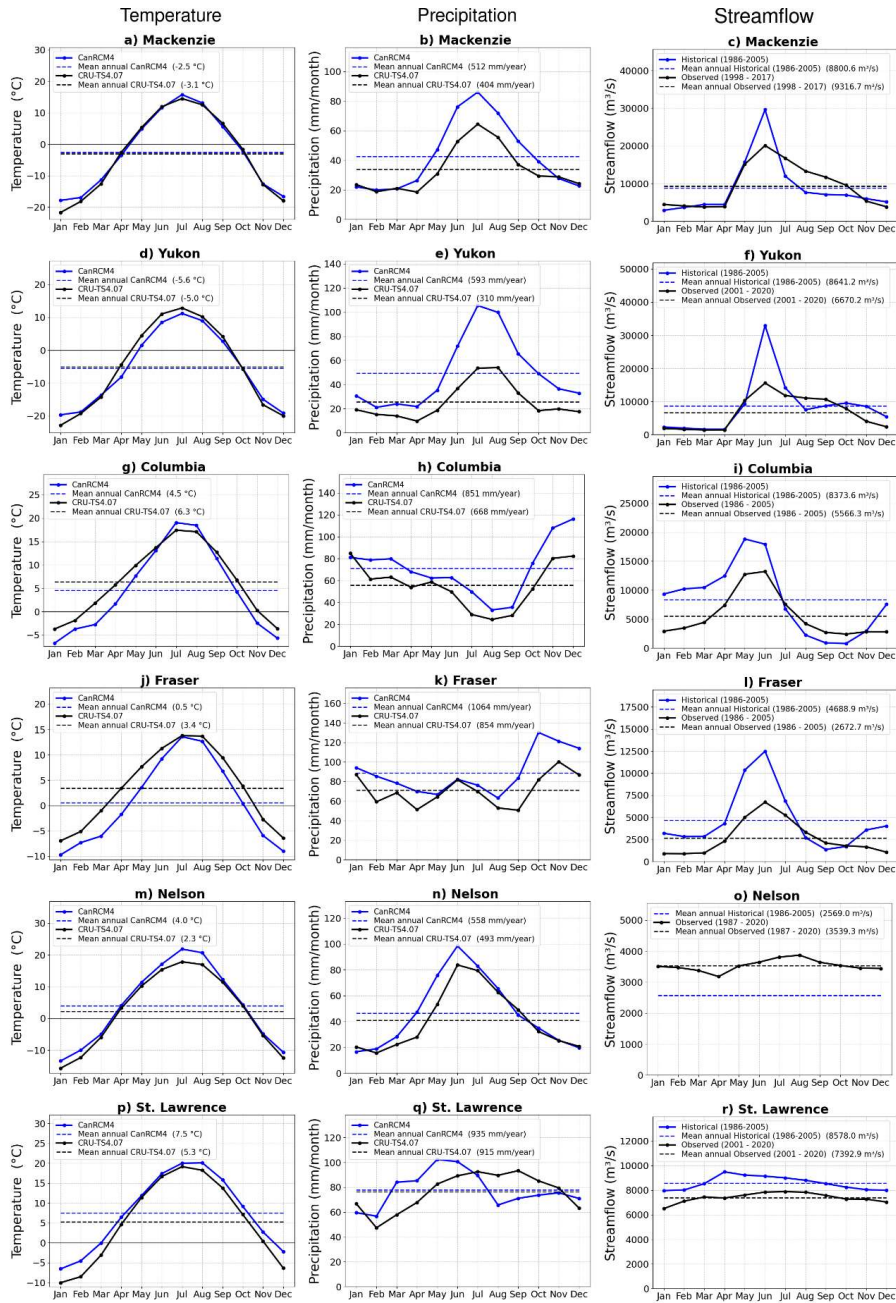
335 Figure 4 compares the simulated annual cycle of temperature (left column) and  
336 precipitation (middle column) over the six river basins (Figure 1) selected in this study with  
337 observation-based estimates from CRU. The right-hand side column compares simulated  
338 streamflow for the six river basins with observation-based estimates from the GRDC. The basin-  
339 averaged values of temperature and precipitation are calculated by area weighting the values in  
340 the individual grid cells that lie inside a given river basin according to the TRIP data (Figure 1).  
341 The plots also show the mean annual values (dashed lines) on the plot and their magnitude in  
342 the legend. Figure 4 shows that overall CanRCM4 simulated basin-wide averaged temperatures  
343 compare reasonably well with observation-based estimates based on the CRU for the Mackenzie  
344 and the Yukon River basins. For the Columbia and Fraser, the simulated temperatures are lower



345 for most months, and for the Nelson River basin, the CanRCM4 simulated temperatures are  
346 higher compared to the CRU data. The seasonal cycle of temperature compares well with the  
347 observation-based estimates from CRU data. Compared to temperature, there are larger  
348 differences in simulated CanRCM4 precipitation compared to the CRU data. Although CanRCM4  
349 simulates the seasonality of precipitation reasonably well compared to the CRU data, simulated  
350 precipitation is higher for all river basins, consistent with Figure 3c. The comparison with the CRU  
351 data provides useful insights into simulated quantities. However, all observation-based data sets  
352 (including CRU) have their limitations. Wong et al. (2017) compared several gridded observation-  
353 based precipitation datasets over Canada and found that they all have limitations and the  
354 datasets compared best with gauge-based precipitation data in summer, followed by autumn,  
355 spring, and winter in order of decreasing quality. Sun et al. (2018) compare global precipitation  
356 from 22 gauge-, satellite-, and reanalysis-based products, including CRU, and quantify the  
357 uncertainty in the different precipitation estimates over timescales ranging from daily to annual.  
358 Shi et al. (2017) evaluated the CRU precipitation over large regions of China and found that CRU  
359 underestimates precipitation in that region compared to rain gauge records. In the end, the  
360 objective of the comparison of the simulated climate with CRU observations is to evaluate if the  
361 model climate is reasonably realistic for the present day. The assumption behind using direct  
362 output from climate models is that despite the biases in the simulated current climate it is  
363 possible to deduce meaningful information about the effect of climate change using the change  
364 in simulated quantities.

365

366



367

368 **Figure 4:** Comparison of the annual cycle of basin-wide averaged CanRCM4 simulated  
 369 temperature (left column) and precipitation (middle column) with observation-based estimates  
 370 from the CRU TS 4.07 dataset for the period 1986-2005. The right-hand side column compares  
 371 simulated streamflow with observations from the GRDC.



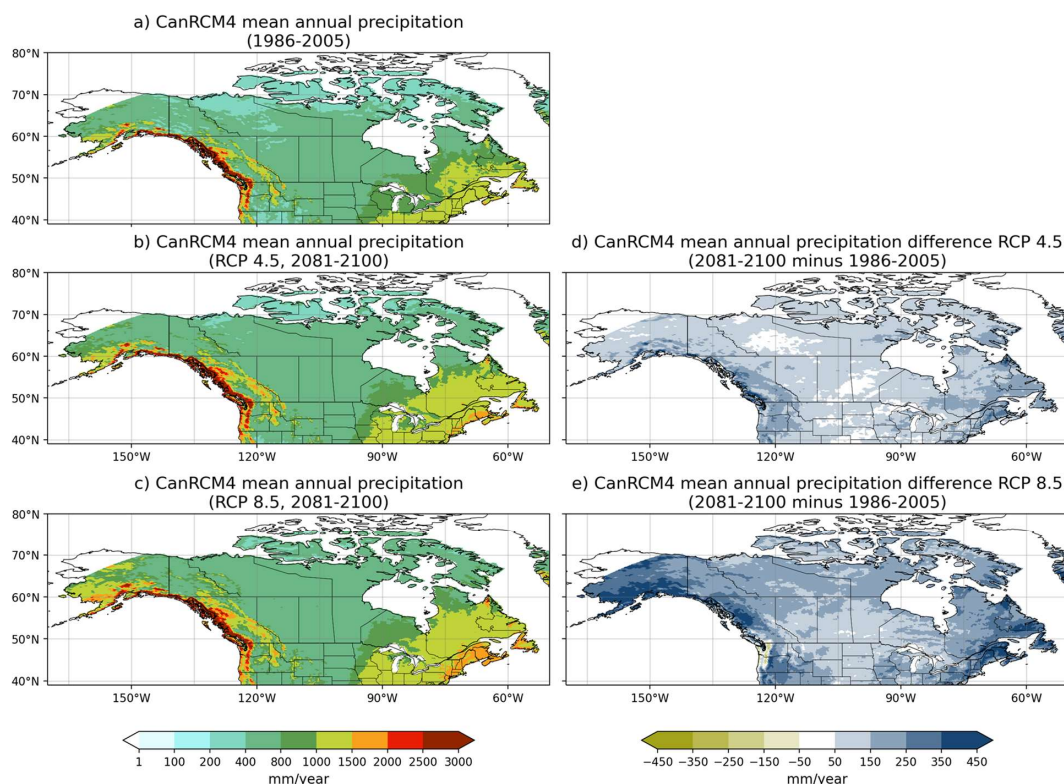
372           The differences in simulated climate for the present day affect simulated streamflow as  
373 expected. The simulated mean annual streamflow is higher for four out of six river basins  
374 considered (Yukon, Columbia, Fraser, and St. Lawrence) primarily because of the higher  
375 simulated precipitation. Simulated precipitation is also higher for the Mackenzie River basin, but  
376 the mean annual simulated streamflow compares well with its observation-based estimate.  
377 Possible reasons for reasonably realistic annual simulated streamflow despite higher  
378 precipitation could be biases in the CRU dataset itself, or higher simulated evaporation in  
379 CanRCM4 (although simulated summer temperatures compare well with the CRU data). Finally,  
380 the simulated mean annual streamflow for the Nelson River is lower than its observation-based  
381 estimate despite somewhat higher simulated precipitation than the CRU data. The most likely  
382 reason for this is the diversion from the Churchill River into the Nelson River which started in  
383 1976 to increase the water flow to larger generating stations on the lower Nelson River. The  
384 Manitoba government estimates that an average of 25% more water flows into the lower Nelson  
385 River due to the Churchill River Diversion (CRD) ([https://www.gov.mb.ca/sd/water/water-  
386 power/churchill/index.html](https://www.gov.mb.ca/sd/water/water-power/churchill/index.html), last accessed Sep. 2023). The seasonality of Mackenzie, Yukon, and  
387 Fraser Rivers is dominated by the spring snowmelt with the peak occurring in June for both  
388 simulated and observed streamflow. The simulated streamflow for the Columbia and Fraser  
389 rivers peaks at the right time but there is more simulated streamflow during the winter months  
390 when precipitation is also higher than observed. For the Mackenzie and Yukon rivers although  
391 the mean annual simulated and observed streamflow are comparable their seasonal distribution  
392 is not. The simulated streamflow peak for these rivers is higher due to the simple treatment of  
393 ice jams which is not sufficient to hold the water in the river channel and then release it slowly



394 as ice jams slowly dissipate in the spring and summer months, as the observed streamflow  
395 indicates. Finally, for the St. Lawrence River, there is little seasonality in observed streamflow  
396 due to the delay caused by the Great Lakes and anthropogenic flow regulation. The lack of strong  
397 seasonality simulated in simulated streamflow for the St. Lawrence River is caused entirely due  
398 to the delay caused by the Great Lakes (section 2.2).

399 Overall the spatial distribution of precipitation and temperature over Canada (Figure 3),  
400 and the seasonality of these two primary climate drivers for the river basins considered in this  
401 study (Figure 4), compare reasonably well with observation-based estimates from the CRU data,  
402 although there are differences in the absolute magnitude of these variables. The resulting  
403 seasonality of streamflow has limitations due to three factors: 1) the biases in the driving climate  
404 from CanRCM4, 2) the biases in the land surface component of CanRCM4 which partitions  
405 precipitation into evaporation and runoff, 3) the lack of calibration of the land surface component  
406 to specific river basins, and 4) the lack of processes in the routing component including the  
407 limitation of not being able to treat ice jams comprehensively. Despite these limitations, the  
408 simulated streamflow captures the broad seasonal patterns with higher values during the spring  
409 snow melt and lower values during the winter months as observations show.

410



411 **Figure 5:** Comparison of CanRCM4 simulated precipitation for the 1986-2005 and 2081-2100  
412 periods, for RCP 4.5 and 8.5 scenarios.

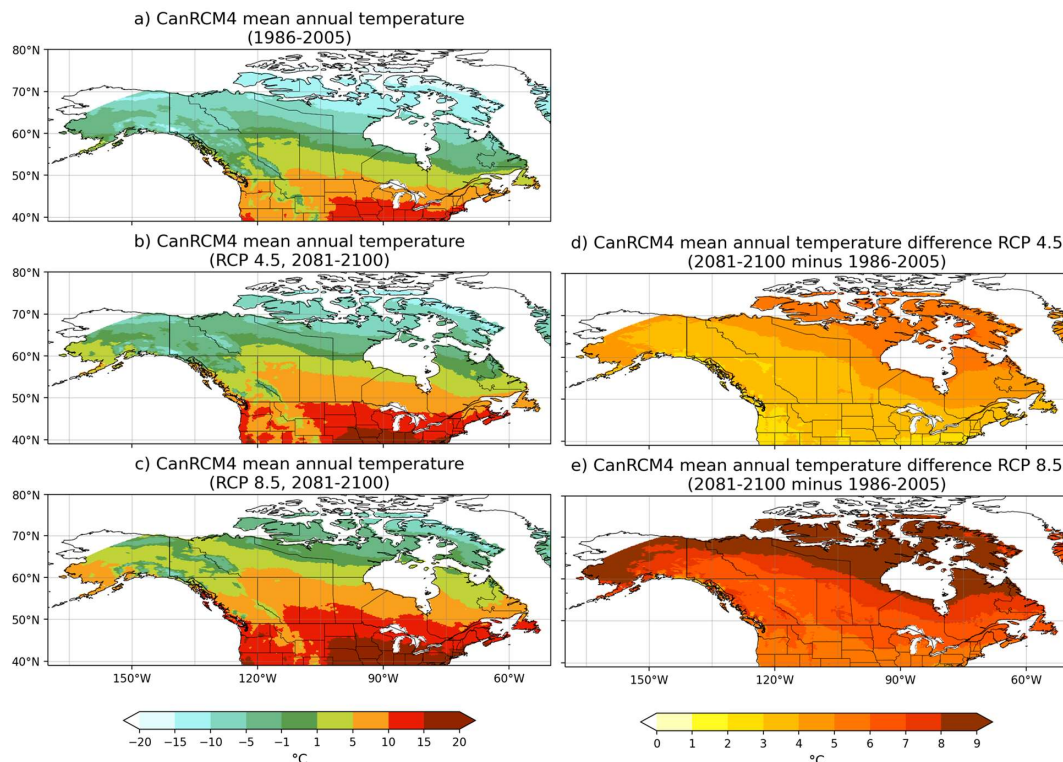
413

### 414 **3.2 Changes in future climate and streamflow**

415 Figures 5, 6, and 7 show the changes in CanRCM4 simulated precipitation, temperature,  
416 and runoff for the period 2081-2100, for both RCP 4.5 and 8.5 scenarios, compared to the 1986-  
417 2005 period from the historical simulation. Over Canada, simulated precipitation and  
418 temperature increase almost everywhere and in both scenarios. As expected, the magnitude of  
419 precipitation and temperature change is higher for the RCP 8.5 than the RCP 4.5 scenario.  
420 Simulated precipitation increases are higher in the coastal western and eastern Canadian regions  
421 than in central and northern parts of Canada. The central Canadian region sees the lowest



422 increase in precipitation in both scenarios. Simulated temperature increases, as expected, are  
423 higher at higher latitudes due to polar amplification of the temperature change associated with  
424 the snow- and ice-albedo feedback. In the RCP 4.5 and 8.5 scenarios, the simulated temperature  
425 changes vary from about 3 °C and 6 °C, respectively, in the south, to about 6 °C and 11 °C, in the  
426 north. The parent climate model (CanESM2) on which CanRCM4 is based has an equilibrium  
427 climate sensitivity of 3.7 °C, somewhat on the higher side, compared to the range of 1.5 °C to 4.5  
428 °C amongst climate models that contributed to CMIP5 (Schlund et al., 2020). As a result, we also  
429 then expect the magnitude of simulated changes to be somewhat higher than a model with  
430 average climate sensitivity.

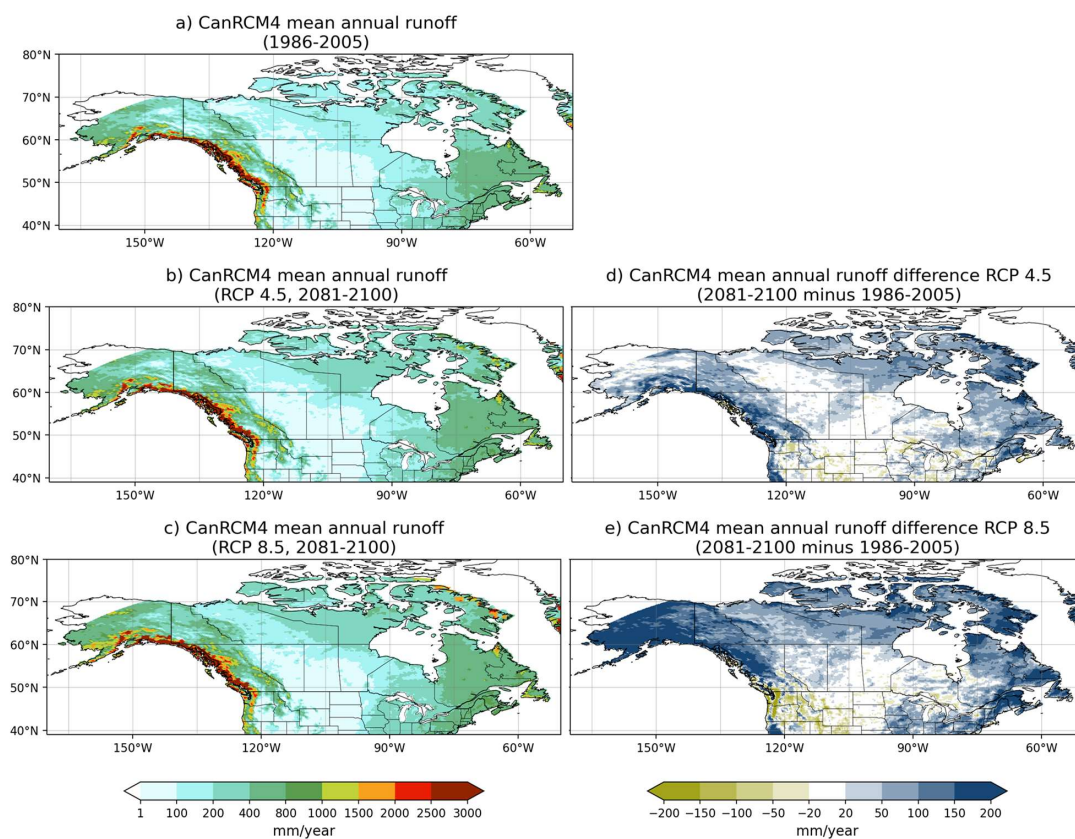


431 **Figure 6:** Comparison of CanRCM4 simulated temperature for the 1986-2005 and 2081-2100  
432 periods, for RCP 4.5 and 8.5 scenarios.





433



434

435 **Figure 7:** Comparison of CanRCM4 simulated runoff for the 1986-2005 and 2081-2100 periods,  
436 for RCP 4.5 and 8.5 scenarios.

437

438 In Figure 7 runoff increases generally everywhere in Canada for the RCP 4.5 and RCP 8.5 scenarios  
439 with larger changes on the west and east coasts, and in northern Canada, following a similar  
440 pattern of changes in precipitation. Runoff reduces in parts of the southern Columbia River basin  
441 in the United States in the RCP 4.5 scenario, and these decreases become more pronounced and  
442 widespread over the north-western Pacific region in the RCP 8.5 scenario including the Fraser  
443 River basin in Canada.



444  
445  
446  
447  
448  
449  
450  
451  
452  
453  
454  
455  
456  
457  
458  
459  
460  
461  
462  
463  
464  
465  
466  
467  
468  
469  
470  
471  
472  
473

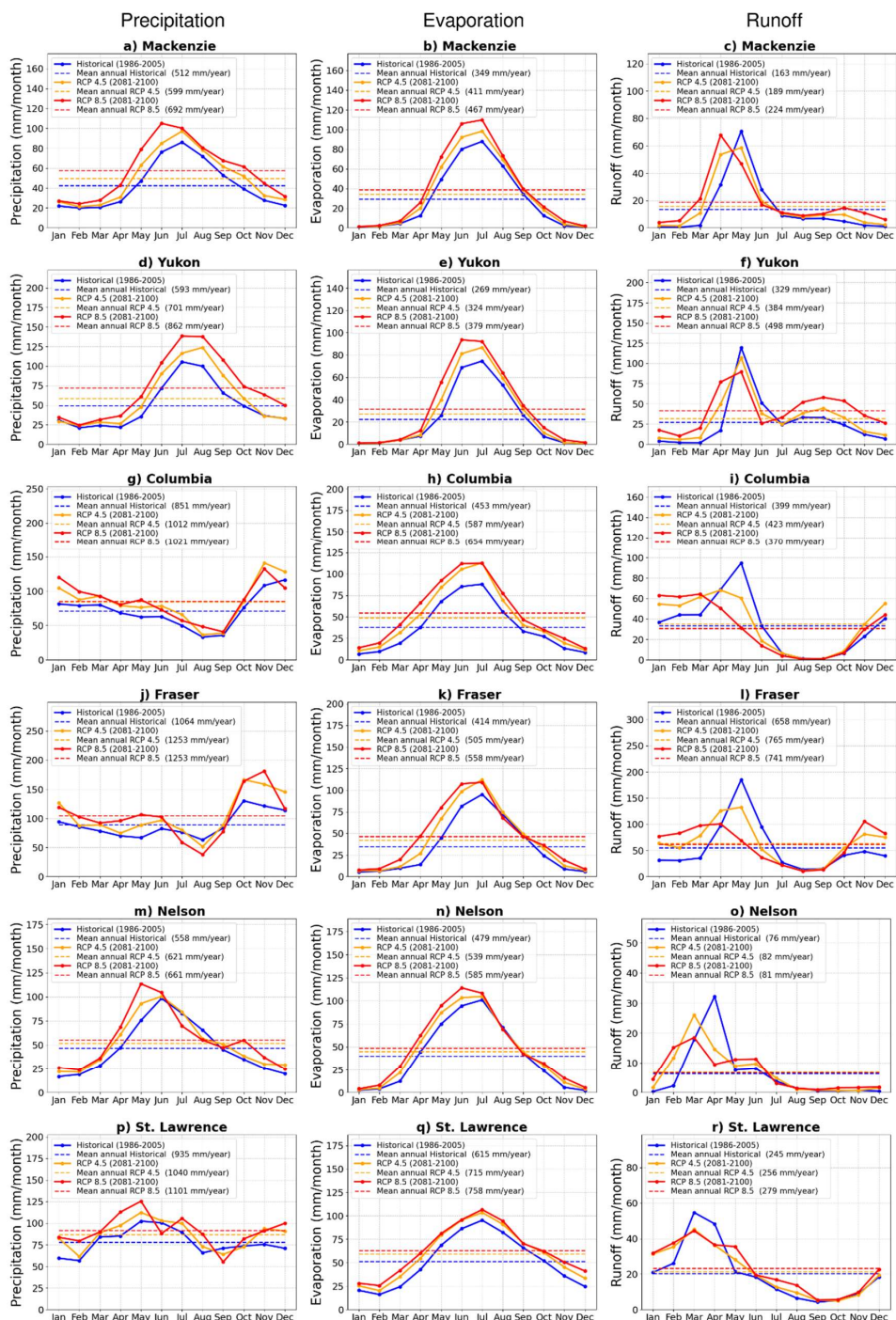


**Figure 8:** Comparison of the annual cycle of basin-wide averaged CanRCM4 simulated water budget components for each river basin for the historical (1986-2005) period and the two future scenarios RCP 4.5 and 8.5 (2081-2100): precipitation (left column), evaporation (middle column), and runoff (right column).



478  
479  
480  
481  
482  
483  
484  
485  
486  
487  
488  
489  
490  
491  
492  
493  
494  
495  
496  
497  
498  
499  
500  
501  
502  
503  
504  
505  
506  
507  
508  
509  
510  
511  
512  
513  
514  
515  
516

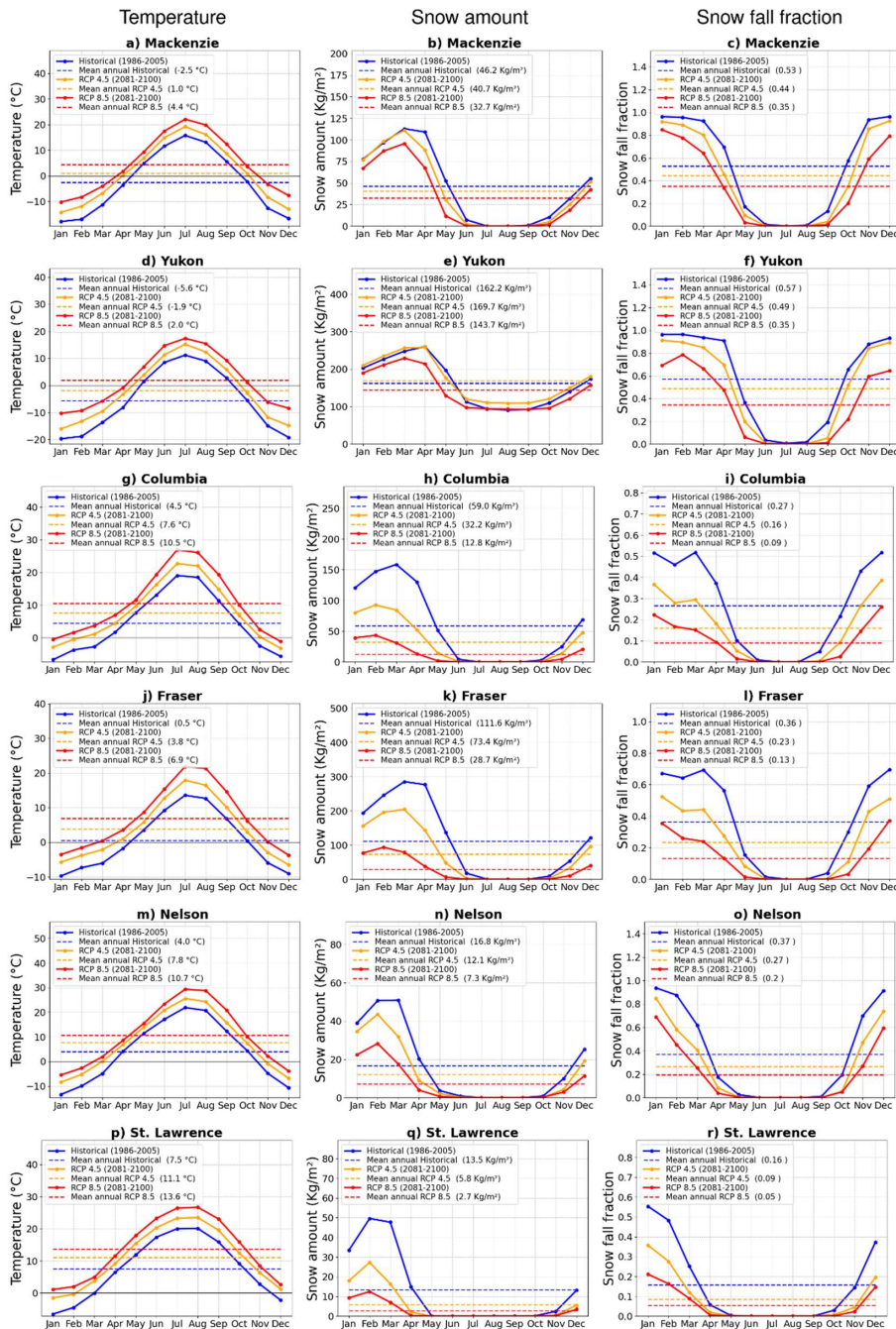


**Figure 9:** Comparison of the annual cycle of basin-wide averaged CanRCM4 simulated temperature (left column), snow water equivalent amount (middle column), and snowfall fraction (right column) for the historical (1986-2005) period and the two future scenarios RCP 4.5 and 8.5 (2081-2100).



521 Figure 8 shows the annual cycle of the simulated water budget components  
 522 (precipitation, evaporation, and runoff) for the six river basins considered in this study for the  
 523 historical (1986-2005) period and the two future scenarios, RCP 4.5 and 8.5 (2081-2100). As in  
 524 Figure 4, the mean annual values are shown as dashed lines and their magnitude is noted in the  
 525 legend.

526 **Table 2:** Evaporation and runoff ratios for the five river basins simulated by CanRCM4 for the  
 527 historical period (1986-2005) and the two future scenarios (RCP 4.5 and 8.5, 2081-2100). The  
 528 evaporation (runoff) ratio is the ratio of mean annual evaporation (runoff) to precipitation.  
 529

River basin	Evaporation ratio (E/P)			Runoff ratio (R/P)		
	Historical (1986-2005)	RCP 4.5 (2081-2100)	RCP 8.5 (2081-2100)	Historical (1986-2005)	RCP 4.5 (2081-2100)	RCP 8.5 (2081-2100)
Mackenzie	0.682	0.686	0.675	0.318	0.316	0.324
Yukon	0.454	0.462	0.440	0.555	0.548	0.579
Columbia	0.532	0.580	0.641	0.469	0.418	0.362
Fraser	0.389	0.403	0.445	0.618	0.611	0.591
Nelson	0.858	0.868	0.885	0.136	0.132	0.123
St. Lawrence	0.664	0.686	0.684	0.314	0.294	0.302

530  
 531 The evaporation (E/P) and runoff (R/P) ratios for the six river basins for the historical period and  
 532 the two future scenarios are shown in Table 2 and allow to see how the partitioning of  
 533 precipitation into evaporation and runoff changes with climate. For the mean annual values of P,  
 534 E, and R reported in Figure 8, P is balanced to within 1% by (E+R) for all river basins (except the  
 535 St. Lawrence) and all scenarios, except for the Yukon (for RCP 8.5) and the Fraser River basins (for  
 536 RCP 4.5 and 8.5) for which (E+R) is higher than P indicating that  $\Delta S$  is not zero (see equation 1).  
 537 As a result, (E/P) and (R/P) also add to one for all river basins except for the Yukon (RCP  
 538 8.5,  $(E + R)/P = 1.02$ ) and the Fraser River (RCP 4.5,  $(E + R)/P = 1.014$ , and RCP 8.5,  
 539  $(E + R)/P = 1.036$ ) basins. For the St. Lawrence River basin, the imbalance is around 2%  
 540 because of the presence of the Great Lakes which had to be excluded from the river basin mask.



541 Since basin-wide averaged calculations are done at 0.5° latitude-longitude resolution, and the  
542 actual domain of CanRCM4 is on rotated latitude-longitude projection this led to slightly more  
543 rounding errors for the St. Lawrence than other river basins.

544 For all river basins considered, precipitation increases for both future scenarios with the  
545 increase being larger for the RCP 8.5 scenario consistent with Figures 5d and 5e. The response of  
546 evaporation to changes in climate is expected. The increase in precipitation and temperature  
547 yields an increase in evaporation for future scenarios for all river basins. Simulated runoff does  
548 not increase as much as precipitation since evaporation also increases. The runoff ratio, in Table  
549 2, increases for the northerly Mackenzie and the Yukon River basins while it decreases for the  
550 southerly Nelson, St. Lawrence, and especially for the Fraser and Columbia River basins which  
551 are characterized by milder climate owing to their location in the Pacific north-western region.  
552 This is because the increase in precipitation is more than enough to compensate for the increase  
553 in evaporation (associated with a warmer climate) for the northern river basins but not for the  
554 southern ones (as seen earlier in Figure 7 where runoff begins to decrease in parts of the  
555 Columbia and Fraser River basins). The absolute runoff amount in Figure 8 increases for the  
556 Mackenzie and Yukon River basins, in the RCP 4.5 and 8.5 scenarios compared to the historical  
557 simulation, but doesn't change much for the Columbia, Fraser, Nelson, and St. Lawrence River  
558 basins. However, the seasonality of runoff changes for all river basins, and simulated runoff peak  
559 either occurs earlier in the year, occurs with reduced magnitude, or both. Canadian rivers are  
560 dominated by spring snowmelt and this runoff behaviour is associated with snow melt occurring  
561 earlier in the year in the RCP 4.5 scenario than in the historical simulation, and occurring earlier  
562 in the RCP 8.5 scenario than in the RCP 4.5 scenario. This is seen in Figure 9 which shows the



563 simulated annual cycle of temperature changes, snow amount, and snowfall as a fraction of total  
564 precipitation for the historical period and the two RCP scenarios for the six river basins. In Figure  
565 9 the mean annual temperature increase from the historical period to the RCP 4.5 scenario, and  
566 from the RCP 4.5 to RCP 8.5 scenario, is between 3 and 3.5 °C for the six river basins considered  
567 here. The middle column of Figure 9 shows that in addition to earlier snowmelt the amount of  
568 snow in the winter months decreases for all river basins with climate warming. The only  
569 exception to this is the Yukon River basin in which the mean annual snow amount increases  
570 marginally in the RCP 4.5 scenario (Figure 9e). As expected, the fraction of precipitation falling as  
571 snow also decreases with climate warming for all river basins (right column, Figure 9).

572

573

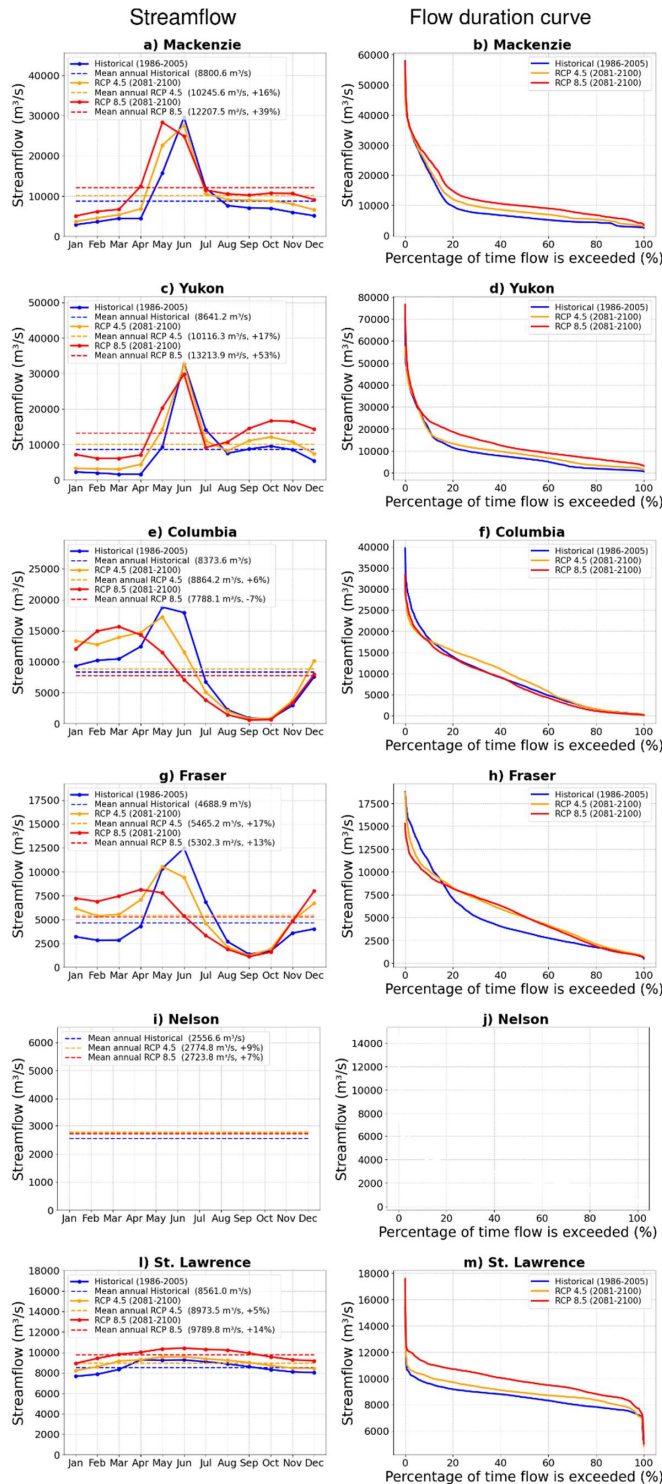
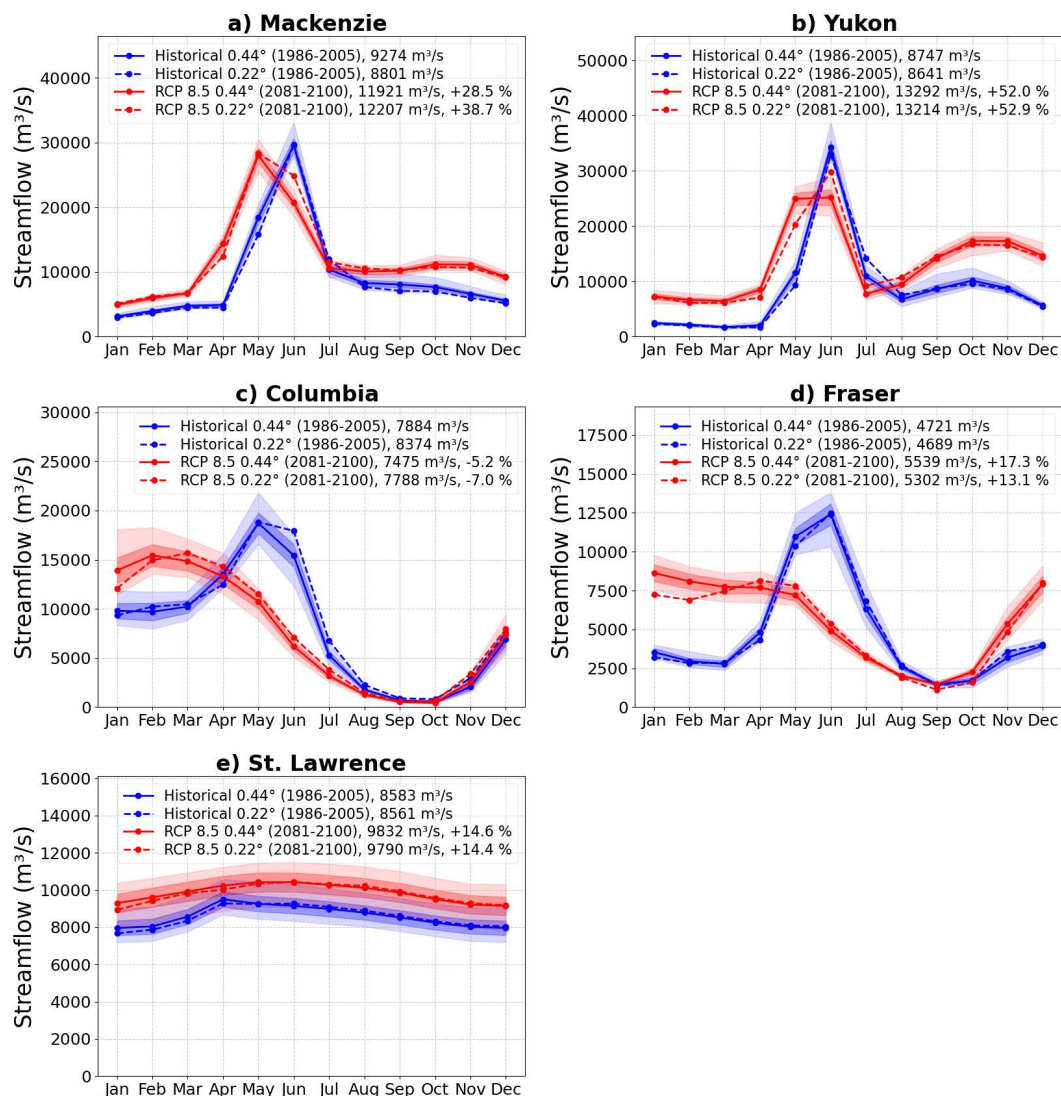


**Figure 10:** Comparison of the simulated monthly streamflow (left column) and flow duration curves (right column) for the historical (1986-2005) period and the two future scenarios RCP 4.5 and 8.5 (2081-2100) for the six river basins considered.



596  
 597 **Figure 11:** Comparison of the simulated monthly streamflow for the historical (1986-2005)  
 598 period and the RCP 8.5 scenario (2081-2100) for the river basins considered in this study from  
 599 the 0.22° and 0.44° simulations. The results from the 0.22° simulations (shown earlier in Figure  
 600 10) are shown as dashed lines. The uncertainty range for the 0.44° simulations is based on  
 601 results from CanRCM4's 50-member large ensemble. The solid lines indicate the mean across  
 602 50 members the light shading indicates the full range, and the dark shading indicates the mean  
 603 ± one standard deviation range, for the 0.44° simulations.





604            Figure 10 compares simulated monthly streamflow and flow duration curves for the  
605            historical (1986-2005) period with those from the two future scenarios RCP 4.5 and 8.5 (2081-  
606            2100) for the six river basins considered. The flow duration curves are calculated using daily  
607            streamflow values. Monthly streamflow and flow duration curves are not shown for the Nelson  
608            River because we do not consider anthropogenic flow regulation, as mentioned earlier. The  
609            legends in Figure 10 for the streamflow figures in the left column show mean annual values but  
610            also the change from the simulated historical values for the RCP 4.5 and 8.5 scenarios. The mean  
611            annual streamflow increases for all rivers for both the RCP 4.5 and 8.5 scenarios, except for the  
612            Columbia River for the RCP 8.5 scenario (-7%). The increase in simulated annual streamflow is  
613            largest for the Mackenzie (+16%, +39%) and Yukon Rivers (+17%, +53%) for the RCP 4.5 and 8.5  
614            scenarios, due to higher precipitation increase in these two basins (Figure 8). The increase in  
615            annual streamflow for other rivers is smaller and between 6% and 14%.

616            The changes in streamflow seasonality are larger for the southerly Columbia and Fraser  
617            Rivers than for the northerly Mackenzie and Yukon Rivers. The peak monthly streamflow for the  
618            Yukon River still occurs in June given it's the coldest river basin (Figure 4d) and the streamflow  
619            seasonality is still dominated by the spring snowmelt. However, despite the peak streamflow still  
620            occurring in June the streamflow does begin to increase earlier due to earlier snowmelt (Figure  
621            9e). While the June streamflow peak doesn't change substantially, streamflow increases for most  
622            other months for the Yukon River. For the Mackenzie River, the peak streamflow occurs in June  
623            in the RCP 4.5 scenario as in the historical simulation but a month earlier in the RCP 8.5 scenario.  
624            Like the Yukon, although the peak streamflow doesn't change substantially for the Mackenzie  
625            River it increases for most other months. These changes in streamflow are also seen in the flow



626 duration curves which show that for these two rivers the frequency of the occurrence of flows  
627 that occur greater than about 5% of the time in the historical simulation increases in the future.  
628 The Columbia and the Fraser Rivers experience much larger changes in their seasonality as their  
629 primarily snow-dominated nival flow regimes change to more hybrid flow regimes. The  
630 snowmelt-driven streamflow peak in spring is reduced considerably for future scenarios since a  
631 lower fraction of fall, winter, and spring precipitation falls as snow. As a result, streamflow  
632 increases from October to April since precipitation falls as rain, as opposed to snow, yields runoff  
633 that runs straight into the rivers. Additionally, the large reduction in snowpack volume together  
634 with earlier melt (Figure 9k and 9h) affects the seasonality of Fraser and Columbia streamflow  
635 and causes pronounced shifts in peak flows. The pronounced changes in the Fraser River basin  
636 peak flow are apparent in its flow duration curve (Figure 10h) which shows a decrease (increase)  
637 in the frequency of streamflow events which occurred less (more) than about 16% of the time  
638 and result in a more equitable streamflow regime with a pronounced reduction in its seasonality.  
639 Simulated streamflow for the St. Lawrence River shows very little seasonality and since annual  
640 streamflow increases for both scenarios, the flow duration curve simply moves up (Figure 10m).

### 641 **3.3 Uncertainty in simulated changes in future streamflow**

642 In addition to the 0.22° simulations for the North American domain, simulation results  
643 are also available from the 50-member large ensemble (LE) of CanRCM4 at 0.44° resolution. The  
644 LE data are, however, only available for the historical simulation and the RCP 8.5 scenario. Similar  
645 to the 0.22° resolution, we regridded the 0.44° runoff at CanRCM4's rotated latitude longitude  
646 projection to 0.5° regular latitude longitude projection for use as input into the river routing



647 scheme. The use of the results from the LE allows us to quantify the uncertainty associated with  
648 streamflow based on the spread in the simulated results associated with the internal variability  
649 of the CanRCM4 model. This is illustrated in Figure 11 which shows the simulated streamflow for  
650 all the rivers considered here except the Nelson River. In Figure 11, the solid lines show the  
651 average across the 50 members of the LE, light shading shows the full range of the results, and  
652 dark shading shows the mean  $\pm$  one standard deviation range (this implies the 5%-95% range  
653 when assuming normally distributed monthly streamflow values). In addition, streamflow from  
654 the 0.22° simulations (from Figure 10) is shown as dashed lines to allow direct comparison of  
655 results from the 0.22° and 0.44° simulations.

656         The changes in simulated streamflow are consistent between the 0.22° and 0.44°  
657 simulations, and for the most part, the results from the 0.22° simulations lie within the full range  
658 of results from the 0.44° simulations. This is expected since the driving climate at the boundaries  
659 of CanRCM4 based on CanESM2 is the same in both resolutions. The exact values and the change  
660 from the historical to the RCP 8.5 scenario (see legend for individual rivers) are, however,  
661 somewhat different. This is also expected since these simulations are different from the 0.22°  
662 simulations. The coarser resolution of the 0.44° simulations implies that the topography is not as  
663 realistically represented as in the 0.22° simulations. In particular, for the Yukon, the results based  
664 on the 0.22° simulation indicate that the month and the magnitude of peak streamflow do not  
665 change significantly in the RCP 8.5 scenario (Figure 10c), while those based on 0.44° suggest that  
666 they do. There are some differences between 0.22° and 0.44° results for the Mackenzie and  
667 Fraser Rivers too. Overall, the LE from the 0.44° simulations helps to provide context for results  
668 from the 0.22° simulations.



669 Overall, despite the differences in the magnitude of changes, the direction and variability  
670 of change obtained from this study is generally consistent with the previous studies using basin-  
671 scale hydrologic models, driven by statistically downscaled and bias-corrected climate model  
672 data, for instance for the Fraser River (Shrestha et al., 2012; Islam et al., 2019), the Columbia  
673 River (Schnorbus et al., 2014) and the Yukon River (Hay and McCabe, 2010). The results presented  
674 here are also comparable to the projections from global and regional scale hydrologic models,  
675 e.g. for the Mackenzie River basin (Krysanova et al., 2017, 2020).

#### 676 **4. Summary and conclusions**

677 This study offers a consistent analysis of results across six river basins in Canada although  
678 based on results from a single climate model. Despite the biases in simulated present-day  
679 CanRCM4 climate, and some differences in the results based on 0.22° and 0.44° simulations, the  
680 results provide useful information about changes in simulated streamflow that is consistent with  
681 expectations of process behaviour in a warmer climate, and with published literature.

682 Neither future precipitation nor temperature changes are uniform across Canada.  
683 Simulated precipitation increases are higher closer to the west and east coasts, and simulated  
684 temperature changes are higher towards the Arctic. Similar to precipitation, runoff changes are  
685 also higher closer to the west and east coasts. The changes in simulated streamflow indicate how  
686 the present-day climate state of river basins plays a role in their response to climate change. The  
687 results yield two broadly distinct responses of monthly streamflow changes to climate warming,  
688 up until the end of this century, for the northerly Mackenzie and Yukon rivers and the southerly  
689 Fraser and Columbia rivers. Despite higher future projected temperature changes in Canada's



690 north, peak streamflow for the Mackenzie and Yukon rivers is still dominated by the spring  
691 snowmelt. This is because the present-day colder states of these river basins imply that even  
692 after around 6-7 °C warming, the basin-wide average temperatures are cold enough to not  
693 sufficiently change their snowmelt-dominated streamflow regimes. Changes, however, do occur  
694 in streamflow seasonality for these two rivers. Peak streamflow month changes from June to May  
695 for the Mackenzie River in the RCP 8.5 scenario for both 0.22° (Figure 9a) and 0.44° (Figure 11a)  
696 simulations and for the Yukon River in the RCP 8.5 scenario for 0.44° simulations (Figure 11b).  
697 Other than the changes in peak month and peak streamflow, snowmelt occurs earlier so  
698 streamflow starts increasing earlier in the spring and the streamflow during the rest of the year  
699 also increases (except for July) due primarily to an increase in precipitation. In contrast, the  
700 streamflow seasonality for the southerly Fraser and Columbia rivers is significantly more affected  
701 by warmer temperatures because the mean annual basin-wide temperature for these river basins  
702 is already above 0° C for the historical period. Both these rivers experience pronounced changes  
703 in their streamflow seasonality. The peak streamflow for both rivers decreases considerably and  
704 occurs two months earlier for the Fraser River and about 2-3 months earlier for the Columbia  
705 River in the RCP 8.5 scenario. These results appear exaggerated compared to the 1-2 months  
706 earlier peak in previous studies for the Fraser (Shrestha et al., 2012; Islam et al., 2019) and  
707 Columbia (Schnorbus et al., 2014) rivers that used results from multiple climate models. Shrestha  
708 et al. (2021a) used CanRCM4 data to evaluate snowpack response to varying degrees of warming.  
709 They found that snowpack reduction using CanRCM4-LE is higher than the ensemble of results  
710 obtained by driving a hydrological model with data from other climate models (their  
711 supplementary information), consistent with CanESM2's higher climate sensitivity.



712           The results presented here also appear to show that the simulated changes in streamflow  
713 are somewhat resolution-dependent. This would be expected especially for topography-  
714 dominated river basins. If a LE of 50 members for the 0.22° resolution was also available, it would  
715 have been easier to draw firm conclusions about the effect of the spatial resolution on changes  
716 in simulated streamflow.

717           There are two primary limitations of the work presented here. First, we use results from  
718 only one climate model. It would have been ideal to use runoff from other regional climate  
719 models to provide an uncertainty range based on the spread across different climate models.  
720 This would also allow us to evaluate how the spread across the models compares to the spread  
721 across the 50 members of the CanRCM4 LE. Second, the results are based on direct output from  
722 the CanRCM4 climate model and direct climate model output is biased. This limitation is tied to  
723 our methodology. Bias-correcting climate data in our case inevitably implies using a different  
724 hydrological model or land surface scheme, than the land surface component of CanRCM4, and  
725 forcing it with bias-corrected climate data to obtain runoff. Finally, there are uncertainties  
726 associated with the routing process itself. As mentioned earlier, the routing scheme accounts for  
727 ice jams in a simplified manner and anthropogenic flow regulation is not taken into account.

728           Large ensembles are now becoming more common. The challenge for similar future  
729 studies is to consider the inter-model and intra-model (based on ensemble members of the same  
730 model) spreads in the same framework to derive an uncertainty estimate that is consistent with  
731 both types of uncertainties.

732  
733



734 **Acknowledgment**

735

736 We thank Daniel Peters for the helpful discussions at the beginning of this work and Sal Curasi  
737 for providing comments on the final version of this manuscript. We also acknowledge the efforts  
738 of the climate modelling team at the Canadian Centre for Climate Modelling and Analysis  
739 (CCCma) who made the results from CanRCM4 available.

740

741 **Code/Data availability**

742

743 The CanRCM4 data from 0.22° simulations used in this study are available from CCCma website  
744 (<https://climate-modelling.canada.ca/climatemodeldata/canrcm/CanRCM4/>). The data from  
745 the 0.44° CanRCM4 large ensemble are available from Environment and Climate Change  
746 Canada (<https://open.canada.ca/data/en/dataset/83aa1b18-6616-405e-9bce-af7ef8c2031c>).  
747

748 **Author contributions**

749

750 VKA designed the study and wrote the majority of the manuscript. AL implemented river  
751 routing to operate at 0.5° resolution and performed all the simulations. RS and AL contributed  
752 to the manuscript text. RS also performed a literature review of existing studies that focus on  
753 the impact of climate change on Canadian rivers.  
754

755 **Competing interests**

756

757 The authors declare that they have no competing interests.  
758

759 **References**

- 760 Alaya, M. A. B., Zwiers, F., and Zhang, X.: Evaluation and Comparison of CanRCM4 and CRCM5 to  
761 Estimate Probable Maximum Precipitation over North America, *J. Hydrometeorol.*, 20, 2069–2089,  
762 <https://doi.org/10.1175/JHM-D-18-0233.1>, 2019.
- 763 Arora, V. K. and Boer, G. J.: Effects of simulated climate change on the hydrology of major river basins, *J.*  
764 *Geophys. Res. Atmospheres*, 106, 3335–3348, <https://doi.org/10.1029/2000JD900620>, 2001.
- 765 Arora, V. K. and Boer, G. J.: A Representation of Variable Root Distribution in Dynamic Vegetation  
766 Models, *Earth Interact.*, 7, 1–19, [https://doi.org/10.1175/1087-3562\(2003\)007<0001:AROVRD>2.0.CO;2](https://doi.org/10.1175/1087-3562(2003)007<0001:AROVRD>2.0.CO;2),  
767 2003.
- 768 Arora, V. K. and Boer, G. J.: A parameterization of leaf phenology for the terrestrial ecosystem  
769 component of climate models, *Glob. Change Biol.*, 11, 39–59, <https://doi.org/10.1111/j.1365-2486.2004.00890.x>, 2005.  
770



- 771 Arora, V. K. and Boer, George. J.: A variable velocity flow routing algorithm for GCMs, *J. Geophys. Res.*  
772 *Atmospheres*, 104, 30965–30979, <https://doi.org/10.1029/1999JD900905>, 1999.
- 773 Arora, V. K. and Harrison, S.: Upscaling river networks for use in climate models, *Geophys. Res. Lett.*, 34,  
774 <https://doi.org/10.1029/2007GL031865>, 2007.
- 775 Arora, V. K., Boer, G. J., Christian, J. R., Curry, C. L., Denman, K. L., Zahariev, K., Flato, G. M., Scinocca, J.  
776 F., Merryfield, W. J., and Lee, W. G.: The Effect of Terrestrial Photosynthesis Down Regulation on the  
777 Twentieth-Century Carbon Budget Simulated with the CCCma Earth System Model, *J. Clim.*, 22, 6066–  
778 6088, <https://doi.org/10.1175/2009JCLI3037.1>, 2009.
- 779 Arora, V. K., Scinocca, J. F., Boer, G. J., Christian, J. R., Denman, K. L., Flato, G. M., Kharin, V. V., Lee, W.  
780 G., and Merryfield, W. J.: Carbon emission limits required to satisfy future representative concentration  
781 pathways of greenhouse gases, *Geophys. Res. Lett.*, 38, n/a-n/a,  
782 <https://doi.org/10.1029/2010GL046270>, 2011.
- 783 Beltaos, S.: Advances in river ice hydrology, *Hydrol. Process.*, 14, 1613–1625,  
784 [https://doi.org/10.1002/1099-1085\(20000630\)14:9<1613::AID-HYP73>3.0.CO;2-V](https://doi.org/10.1002/1099-1085(20000630)14:9<1613::AID-HYP73>3.0.CO;2-V), 2000.
- 785 Bonsal, B., Shrestha, R. R., Dibike, Y., Peters, D. L., Spence, C., Mudryk, L., and Yang, D.: Western  
786 Canadian Freshwater Availability: Current and Future Vulnerabilities, *Environ. Rev.*, 28, 528–545,  
787 <https://doi.org/10.1139/er-2020-0040>, 2020.
- 788 Budhathoki, S., Rokaya, P., and Lindenschmidt, K.-E.: Impacts of future climate on the hydrology of a  
789 transboundary river basin in northeastern North America, *J. Hydrol.*, 605, 127317,  
790 <https://doi.org/10.1016/j.jhydrol.2021.127317>, 2022.
- 791 Chen, Y. and She, Y.: Long-term variations of river ice breakup timing across Canada and its response to  
792 climate change, *Cold Reg. Sci. Technol.*, 176, 103091,  
793 <https://doi.org/10.1016/j.coldregions.2020.103091>, 2020.
- 794 Côté, J., Gravel, S., Méthot, A., Patoine, A., Roch, M., and Staniforth, A.: The Operational CMC–MRB  
795 Global Environmental Multiscale (GEM) Model. Part I: Design Considerations and Formulation, *Mon.*  
796 *Weather Rev.*, 126, 1373–1395, [https://doi.org/10.1175/1520-0493\(1998\)126<1373:TOCMGE>2.0.CO;2](https://doi.org/10.1175/1520-0493(1998)126<1373:TOCMGE>2.0.CO;2),  
797 1998.
- 798 Deser, C., Lehner, F., Rodgers, K. B., Ault, T., Delworth, T. L., DiNezio, P. N., Fiore, A., Frankignoul, C.,  
799 Fyfe, J. C., Horton, D. E., Kay, J. E., Knutti, R., Lovenduski, N. S., Marotzke, J., McKinnon, K. A., Minobe, S.,  
800 Randerson, J., Screen, J. A., Simpson, I. R., and Ting, M.: Insights from Earth system model initial-  
801 condition large ensembles and future prospects, *Nat. Clim. Change*, 10, 277–286,  
802 <https://doi.org/10.1038/s41558-020-0731-2>, 2020.
- 803 Dibike, Y., Muhammad, A., Shrestha, R. R., Spence, C., Bonsal, B., de Rham, L., Rowley, J., Evenson, G.,  
804 and Stadnyk, T.: Application of dynamic contributing area for modelling the hydrologic response of the  
805 Assiniboine River basin to a changing climate, *J. Gt. Lakes Res.*, 47, 663–676,  
806 <https://doi.org/10.1016/j.jglr.2020.10.010>, 2021.
- 807 ECCC: The Canadian Regional Climate Model Large Ensemble. Environment and Climate Change Canada  
808 (ECCC), Government of Canada Open Data Portal. Available at:





- 809 <https://open.canada.ca/data/en/dataset/83aa1b18-6616-405e-9bce-af7ef8c2031c>, Gatineau, QC,  
810 Canada, 2018.
- 811 Gosling, S. N., Taylor, R. G., Arnell, N. W., and Todd, M. C.: A comparative analysis of projected impacts  
812 of climate change on river runoff from global and catchment-scale hydrological models, *Hydrol. Earth  
813 Syst. Sci.*, 15, 279–294, <https://doi.org/10.5194/hess-15-279-2011>, 2011.
- 814 Harris, I., Osborn, T. J., Jones, P., and Lister, D.: Version 4 of the CRU TS monthly high-resolution gridded  
815 multivariate climate dataset, *Sci. Data*, 7, 109, <https://doi.org/10.1038/s41597-020-0453-3>, 2020.
- 816 Hay, L. E. and McCabe, G. J.: Hydrologic effects of climate change in the Yukon River Basin, *Clim. Change*,  
817 100, 509–523, <https://doi.org/10.1007/s10584-010-9805-x>, 2010.
- 818 Hewitson, B. C., Daron, J., Crane, R. G., Zermoglio, M. F., and Jack, C.: Interrogating empirical-statistical  
819 downscaling, *Clim. Change*, 122, 539–554, <https://doi.org/10.1007/s10584-013-1021-z>, 2014.
- 820 Islam, S. U., Curry, C. L., Déry, S. J., and Zwiers, F. W.: Quantifying projected changes in runoff variability  
821 and flow regimes of the Fraser River Basin, British Columbia, *Hydrol. Earth Syst. Sci.*, 23, 811–828,  
822 <https://doi.org/10.5194/hess-23-811-2019>, 2019.
- 823 Ismail, H., Rowshon, M. K., Hin, L. S., Abdullah, A. F. B., and Nasidi, N. M.: Assessment of climate change  
824 impact on future streamflow at Bernam river basin Malaysia, *IOP Conf. Ser. Earth Environ. Sci.*, 540,  
825 012040, <https://doi.org/10.1088/1755-1315/540/1/012040>, 2020.
- 826 Kourzeneva, E., Asensio, H., Martin, E., and Faroux, S.: Global gridded dataset of lake coverage and lake  
827 depth for use in numerical weather prediction and climate modelling, *Tellus Dyn. Meteorol. Oceanogr.*,  
828 <https://doi.org/10.3402/tellusa.v64i0.15640>, 2012.
- 829 Krysanova, V., Vetter, T., Eisner, S., Huang, S., Pechlivanidis, I., Michael Strauch, Gelfan, A., Kumar, R.,  
830 Aich, V., Arheimer, B., Chamorro, A., Griensven, A. van, Kundu, D., Lobanova, A., Mishra, V., Plötner, S.,  
831 Reinhardt, J., Ousmane Seidou, Wang, X., Wortmann, M., Zeng, X., and Hattermann, F. F.:  
832 Intercomparison of regional-scale hydrological models and climate change impacts projected for 12  
833 large river basins worldwide—a synthesis, *Environ. Res. Lett.*, 12, 105002, <https://doi.org/10.1088/1748-9326/aa8359>, 2017.
- 835 Krysanova, V., Zaherpour, J., Didovets, I., Gosling, S. N., Gerten, D., Hanasaki, N., Müller Schmied, H.,  
836 Pokhrel, Y., Satoh, Y., Tang, Q., and Wada, Y.: How evaluation of global hydrological models can help to  
837 improve credibility of river discharge projections under climate change, *Clim. Change*, 163, 1353–1377,  
838 <https://doi.org/10.1007/s10584-020-02840-0>, 2020.
- 839 Lange, S.: Trend-preserving bias adjustment and statistical downscaling with ISIMIP3BASD (v1. 0),  
840 *Geosci. Model Dev.*, 12, 2019.
- 841 MacDonald, M. K., Stadnyk, T. A., Déry, S. J., Braun, M., Gustafsson, D., Isberg, K., and Arheimer, B.:  
842 Impacts of 1.5 and 2.0 °C Warming on Pan-Arctic River Discharge Into the Hudson Bay Complex Through  
843 2070, *Geophys. Res. Lett.*, 45, 7561–7570, <https://doi.org/10.1029/2018GL079147>, 2018.
- 844 Maraun, D.: Bias Correcting Climate Change Simulations - a Critical Review, *Curr. Clim. Change Rep.*, 2,  
845 211–220, <https://doi.org/10.1007/s40641-016-0050-x>, 2016.



- 846 Maraun, D., Shepherd, T. G., Widmann, M., Zappa, G., Walton, D., Gutiérrez, J. M., Hagemann, S.,  
847 Richter, I., Soares, P. M. M., Hall, A., and Mearns, L. O.: Towards process-informed bias correction of  
848 climate change simulations, *Nat. Clim. Change*, 7, 764–773, <https://doi.org/10.1038/nclimate3418>,  
849 2017.
- 850 Miller, J. R. and Russell, G. L.: The impact of global warming on river runoff, *J. Geophys. Res.*  
851 *Atmospheres*, 97, 2757–2764, <https://doi.org/10.1029/91JD01700>, 1992.
- 852 Miller, O. L., Putman, A. L., Alder, J., Miller, M., Jones, D. K., and Wise, D. R.: Changing climate drives  
853 future streamflow declines and challenges in meeting water demand across the southwestern United  
854 States, *J. Hydrol. X*, 11, 100074, <https://doi.org/10.1016/j.hydroa.2021.100074>, 2021.
- 855 Moss, R. H., Edmonds, J. A., Hibbard, K. A., Manning, M. R., Rose, S. K., van Vuuren, D. P., Carter, T. R.,  
856 Emori, S., Kainuma, M., Kram, T., Meehl, G. A., Mitchell, J. F. B., Nakicenovic, N., Riahi, K., Smith, S. J.,  
857 Stouffer, R. J., Thomson, A. M., Weyant, J. P., and Wilbanks, T. J.: The next generation of scenarios for  
858 climate change research and assessment, *Nature*, 463, 747–756, <https://doi.org/10.1038/nature08823>,  
859 2010.
- 860 Oki, T. and Sud, Y. C.: Design of Total Runoff Integrating Pathways (TRIP)—A Global River Channel  
861 Network, *Earth Interact.*, 2, 1–37, [https://doi.org/10.1175/1087-3562\(1998\)002<0001:DOTRIP>2.3.CO;2](https://doi.org/10.1175/1087-3562(1998)002<0001:DOTRIP>2.3.CO;2),  
862 1998.
- 863 Prowse, T. D.: Ice jam characteristics, Liard–Mackenzie rivers confluence, *Can. J. Civ. Eng.*, 13, 653–665,  
864 <https://doi.org/10.1139/l86-100>, 1986.
- 865 Quinn, F. H.: Hydraulic Residence Times for the Laurentian Great Lakes, *J. Gt. Lakes Res.*, 18, 22–28,  
866 [https://doi.org/10.1016/S0380-1330\(92\)71271-4](https://doi.org/10.1016/S0380-1330(92)71271-4), 1992.
- 867 von Salzen, K., Scinocca, J. F., McFarlane, N. A., Li, J., Cole, J. N. S., Plummer, D., Verseghy, D., Reader, M.  
868 C., Ma, X., Lazare, M., and Solheim, L.: The Canadian Fourth Generation Atmospheric Global Climate  
869 Model (CanAM4). Part I: Representation of Physical Processes, *Atmosphere-Ocean*, 51, 104–125,  
870 <https://doi.org/10.1080/07055900.2012.755610>, 2013.
- 871 Schlund, M., Lauer, A., Gentine, P., Sherwood, S. C., and Eyring, V.: Emergent constraints on equilibrium  
872 climate sensitivity in CMIP5: do they hold for CMIP6?, *Earth Syst. Dyn.*, 11, 1233–1258,  
873 <https://doi.org/10.5194/esd-11-1233-2020>, 2020.
- 874 Schnorbus, M., Werner, A., and Bennett, K.: Impacts of climate change in three hydrologic regimes in  
875 British Columbia, Canada, *Hydrol. Process.*, 28, 1170–1189, <https://doi.org/10.1002/hyp.9661>, 2014.
- 876 Scinocca, J. F., Kharin, V. V., Jiao, Y., Qian, M. W., Lazare, M., Solheim, L., Flato, G. M., Biner, S.,  
877 Desgagne, M., and Dugas, B.: Coordinated Global and Regional Climate Modeling, *J. Clim.*, 29, 17–35,  
878 <https://doi.org/10.1175/JCLI-D-15-0161.1>, 2016.
- 879 Shi, H., Li, T., and Wei, J.: Evaluation of the gridded CRU TS precipitation dataset with the point  
880 raingauge records over the Three-River Headwaters Region, *J. Hydrol.*, 548, 322–332,  
881 <https://doi.org/10.1016/j.jhydrol.2017.03.017>, 2017.



- 882 Shrestha, R. R., Schnorbus, M. A., Werner, A. T., and Berland, A. J.: Modelling spatial and temporal  
883 variability of hydrologic impacts of climate change in the Fraser River basin, British Columbia, Canada,  
884 *Hydrol. Process.*, 26, 1840–1860, <https://doi.org/10.1002/hyp.9283>, 2012.
- 885 Shrestha, R. R., Cannon, A. J., Schnorbus, M. A., and Alford, H.: Climatic Controls on Future Hydrologic  
886 Changes in a Subarctic River Basin in Canada, *J. Hydrometeorol.*, 20, 1757–1778,  
887 <https://doi.org/10.1175/JHM-D-18-0262.1>, 2019.
- 888 Shrestha, R. R., Bonsal, B. R., Bonnyman, J. M., Cannon, A. J., and Najafi, M. R.: Heterogeneous snowpack  
889 response and snow drought occurrence across river basins of northwestern North America under 1.0°C  
890 to 4.0°C global warming, *Clim. Change*, 164, 40, <https://doi.org/10.1007/s10584-021-02968-7>, 2021a.
- 891 Shrestha, R. R., Bonsal, B. R., Kayastha, A., Dibike, Y. B., and Spence, C.: Snowpack response in the  
892 Assiniboine-Red River basin associated with projected global warming of 1.0 °C to 3.0 °C, *J. Gt. Lakes  
893 Res.*, 47, 677–689, <https://doi.org/10.1016/j.jglr.2020.04.009>, 2021b.
- 894 Sobie, S. R. and Murdock, T. Q.: Projections of Snow Water Equivalent Using a Process-Based Energy  
895 Balance Snow Model in Southwestern British Columbia, *J. Appl. Meteorol. Climatol.*, 61, 77–95,  
896 <https://doi.org/10.1175/JAMC-D-20-0260.1>, 2022.
- 897 Stadnyk, T. A., Tefs, A., Broesky, M., Déry, S. J., Myers, P. G., Ridenour, N. A., Koenig, K., Vonderbank, L.,  
898 and Gustafsson, D.: Changing freshwater contributions to the Arctic: A 90-year trend analysis (1981–  
899 2070), *Elem. Sci. Anthr.*, 9, <https://doi.org/10.1525/elementa.2020.00098>, 2021.
- 900 Sun, Q., Miao, C., Duan, Q., Ashouri, H., Sorooshian, S., and Hsu, K.-L.: A Review of Global Precipitation  
901 Data Sets: Data Sources, Estimation, and Intercomparisons, *Rev. Geophys.*, 56, 79–107,  
902 <https://doi.org/10.1002/2017RG000574>, 2018.
- 903 Swart, N. C., Cole, J. N. S., Kharin, V. V., Lazare, M., Scinocca, J. F., Gillett, N. P., Anstey, J., Arora, V.,  
904 Christian, J. R., Hanna, S., Jiao, Y., Lee, W. G., Majaess, F., Saenko, O. A., Seiler, C., Seinen, C., Shao, A.,  
905 Sigmund, M., Solheim, L., von Salzen, K., Yang, D., and Winter, B.: The Canadian Earth System Model  
906 version 5 (CanESM5.0.3), *Geosci. Model Dev.*, 12, 4823–4873, [https://doi.org/10.5194/gmd-12-4823-  
907 2019](https://doi.org/10.5194/gmd-12-4823-907), 2019.
- 908 Thrasher, B., Xiong, J., Wang, W., Melton, F., Michaelis, A., and Nemani, R.: Downscaled Climate  
909 Projections Suitable for Resource Management, *Eos Trans. Am. Geophys. Union*, 94, 321–323,  
910 <https://doi.org/10.1002/2013EO370002>, 2013.
- 911 Trenberth, K. E., Smith, L., Qian, T., Dai, A., and Fasullo, J.: Estimates of the Global Water Budget and Its  
912 Annual Cycle Using Observational and Model Data, *J. Hydrometeorol.*, 8, 758–769,  
913 <https://doi.org/10.1175/JHM600.1>, 2007.
- 914 Versegny, D. L.: Class—A Canadian land surface scheme for GCMS. I. Soil model, *Int. J. Climatol.*, 11,  
915 111–133, <https://doi.org/10.1002/joc.3370110202>, 1991.
- 916 Versegny, D. L., McFarlane, N. A., and Lazare, M.: Class—A Canadian land surface scheme for GCMS, II.  
917 Vegetation model and coupled runs, *Int. J. Climatol.*, 13, 347–370,  
918 <https://doi.org/10.1002/joc.3370130402>, 1993.



- 919 Wong, J. S., Razavi, S., Bonsal, B. R., Wheeler, H. S., and Asong, Z. E.: Inter-comparison of daily  
920 precipitation products for large-scale hydro-climatic applications over Canada, *Hydrol. Earth Syst. Sci.*,  
921 21, 2163–2185, <https://doi.org/10.5194/hess-21-2163-2017>, 2017.
- 922 Yoosefdoost, I., Khashei-Siuki, A., Tabari, H., and Mohammadrezapour, O.: Runoff Simulation Under  
923 Future Climate Change Conditions: Performance Comparison of Data-Mining Algorithms and Conceptual  
924 Models, *Water Resour. Manag.*, 36, 1191–1215, <https://doi.org/10.1007/s11269-022-03068-6>, 2022.
- 925 Zhang, X., Tang, Q., Zhang, X., and Lettenmaier, D. P.: Runoff sensitivity to global mean temperature  
926 change in the CMIP5 Models, *Geophys. Res. Lett.*, 41, 5492–5498,  
927 <https://doi.org/10.1002/2014GL060382>, 2014.
- 928
- 929